MitoEAGLE preprint 2018-01-30(20)

The protonmotive force and respiratory control: Building blocks of mitochondrial physiology Part 1.

http://www.mitoeagle.org/index.php/MitoEAGLE_preprint_2017-09-21
Preprint version 20 (2018-01-30)

MitoEAGLE Network
Corresponding author: Gnaiger E
Contributing co-authors
Ahn B, Alves MG, Amati F, Aral C, Arandarčikaitė O, Åsander Frostner E, Bailey DM, Bastos Sant'Anna Silva AC, Battino M, Beard DA, Ben-Shachar D, Bishop D, Breton S, Brown GC, Brown RA, Buettner GR, Calabria E, Cardoso LHD, Carvalho E, Casado Pinna M, Cervinkova Z, Chang SC, Chicco AJ, Chinopoulos C, Coen PM, Collins JL, Crisóstomo L, Davis MS, Dias T, Distefano G, Doerrier C, Drahota Z, Duchen MR, Ehinger J, Elmer E, Endlicher R, Fell DA, Ferko M, Ferreira JCB, Filipovska A, Fisar Z, Fisher J, Garcia-Roves PM, Garcia-Souza LF, Genova ML, Gonzalo H, Goodpaster BH, Gorr TA, Grefte S, Han J, Harrison DK, Hellgren KT, Hernansanz P, Holland O, Hoppel CL, Houstek J, Hunger M, Iglesias-Gonzalez J, Irving BA, Iyer S, Jackson CB, Jansen-Dürr P, Jespersen NR, Jha RK, Kaambre T, Kane DA, Kappler L, Karabatsiakis A, Keijer J, Keppner G, Komlodi T, Kopitar-Jerala N, Krako Jakovljevic N, Kuang J, Kucera O, Labieniec-Watala M, Lai N, Laner V, Larsen TS, Lee HK, Lemieux H, Lerfall J, Lucchinetti E, MacMillan-Crow LA, Makrecka-Kuka M, Meszaros AT, Michalak S, Moisoi N, Molina AJA, Montaigne D, Moore AL, Moreira BP, Mracek T, Muntane J, Muntean DM, Murray AJ, Nedergaard J, Nemec M, Newsom S, Nozickova K, O'Gorman D, Oliveira PF, Oliveira PJ, Orynbayeva Z, Pak YK, Palmeira CM, Patel HH, Pecina P, Pereira da Silva Grilo da Silva F, Pesta D, Petit PX, Pichaud N, Pirkmajer S, Porter RK, Pranger F, Prochownik EV, Puurand M, Radenkovic F, Reboredo P, Renner-Sattler K, Robinson MM, Rohlena J, Røsland GV, Rossiter HB, Rybacka-Mossakowska J, Salvadego D, Scatena R, Schartner M, Scheibye-Knudsen M, Schilling JM, Schlattner U, Schoenfeld P, Scott GR, Shabalina IG, Shevchuk I, Siewiera K, Singer D, Sobotka O, Spinazzi M, Stankova P, Stier A, Stocker R, Sumbalova Z, Suravajhala P, Tanaka M, Tandler B, Tepp K, Tomar D, Towheed A, Tretter L, Trivigno C, Tronstad KJ, Trougakos IP, Tyrrell DJ, Urban T, Velika B, Vendelin M, Vercesi AE, Victor VM, Villena JA, Wagner BA, Ward ML, Watala C, Wei YH, Wieckowski MR, Wohlwend M, Wolff J, Wuest RCI, Zaugg K, Zaugg M, Zorzano A

Supporting co-authors:
Bakker BM, Bernardi P, Boetker HE, Borsheim E, Borutaitė V, Bouitbir J, Calbet JA, Calzia E, Chaurasia B, Clementi E, Coker RH, Collin A, Das AM, De Palma C, Dubouchaud H, Durham WJ, Dyrstad SE, Engin AB, Fornaro M, Gan Z, Garlid KD, Garten A, Gourlay CW, Granata C, Haas CB, Haavik J, Haendeler J, Hand SC, Hepple RT, Hickey AJ, Hoel F, Jang DH, Kainulainen H, Khamoui AV, Klingenspor M, Koopman WJH, Kowaltowski AJ, Krajcova A, Lane N, Lenaz G, Malik A, Markova M, Mazat JP, Menze MA, Methner A, Muntané J, Neuzil J, Oliveira MT, Pallotta ML, Parajuli N, Pettersen IKN, Porter C, Pulinilkunnil T, Ropelle ER, Salin K, Sandi C, Sazanov LA, Silber AM, Skolik R, Smenes BT, Soares FAA, Sokolova I, Sonkar VK, Swerdlow RH, Szabo I, Trifunovic A, Thyfault JP, Valentine JM, Vieyra A, Votion DM, Williams C, Zischka H

Updates:
http://www.mitoeagle.org/index.php/MitoEAGLE_preprint_2017-09-21

Correspondence: Gnaiger E
Department of Visceral, Transplant and Thoracic Surgery, D. Swarovski Research Laboratory, Medical University of Innsbruck, Innrain 66/4, A-6020 Innsbruck, Austria
Email: erich.gnaiger@i-med.ac.at
Tel: +43 512 566796, Fax: +43 512 566796 20

This manuscript on 'The protonmotive force and respiratory control' is a position statement in the frame of COST Action CA15203 MitoEAGLE. The list of co-authors evolved beyond ***phase 1*** *(phase 1 versions 1-44) in the* ***bottom-up*** *spirit of COST.*

This is an open invitation to scientists and students to join as co-authors, to provide a balanced view on mitochondrial respiratory control, a fundamental introductory presentation of the concept of the protonmotive force, and a consensus statement on reporting data of mitochondrial respiration in terms of metabolic flows and fluxes.

Phase 2: *MitoEAGLE preprint (Versions 01 – 16): We continue to invite comments and suggestions, particularly if you are an* ***early career investigator adding an open future-oriented perspective****, or an* ***established scientist providing a balanced historical basis****. Your critical input into the quality of the manuscript will be most welcome, improving our aims to be educational, general, consensus-oriented, and practically helpful for students working in mitochondrial respiratory physiology.*

Phase 3 (2017-11-11) Print version forMiP2017 and MitoEAGLE workshop in Hradec Kralove*:*

» http://www.mitoeagle.org/index.php/MiP2017_Hradec_Kralove_CZ

Discussion of manuscript submission to a preprint server, such as BioRxiv; invite further opinion leaders: *To join as a co-author, please feel free to focus on a particular section in terms of direct input and references, contributing to the scope of the manuscript from the perspective of your expertise. Your comments will be largely posted on the discussion page of the MitoEAGLE preprint website.*

If you prefer to submit comments in the format of a referee's evaluation rather than a contribution as a co-author, I will be glad to distribute your views to the updated list of co-authors for a balanced response. We would ask for your consent on this open bottom-up policy.

Phase 4*: Journal submission. We plan a series of follow-up reports by the expanding MitoEAGLE Network, to increase the scope of recommendations on harmonization and facilitate global communication and collaboration. Further discussions: MitoEAGLE Working Group Meetings, various conferences (EBEC 2018 in Budapest).*

I thank you in advance for your feedback.
With best wishes,

Erich Gnaiger

Chair Mitochondrial Physiology Society - http://www.mitophysiology.org
Chair COST Action MitoEAGLE - http://www.mitoeagle.org

Contents

Abstract Clarity of concept and consistency of nomenclature are key trademarks of a research field. These trademarks facilitate effective transdisciplinary communication, education, and ultimately further discovery. As the knowledge base and importance of mitochondrial physiology to human health expand, the necessity for harmonizing nomenclature concerning mitochondrial respiratory states and rates has become increasingly apparent. Peter Mitchell's chemiosmotic theory establishes the links between electric and chemical components of energy transformation and coupling in oxidative phosphorylation. The unifying concept of the protonmotive force provides the framework for developing a consistent theory and nomenclature for mitochondrial physiology and bioenergetics. Herein, we follow IUPAC guidelines on general terms of physical chemistry, extended by considerations on open systems and irreversible thermodynamics. The protonmotive force is not a force as defined in physics. This conflict is resolved by the generalized formulation of isomorphic forces in energy transformations. We align the nomenclature and symbols of classical bioenergetics with a concept-driven constructive terminology to express the meaning of each quantity clearly and consistently. Uniform standards for evaluation of respiratory states and rates will ultimately support the development of databases of mitochondrial respiratory function in species, tissues, and cells studied under diverse physiological and experimental conditions. In this position statement, in the frame of COST Action MitoEAGLE, we endeavour to provide a balanced view on mitochondrial respiratory control, a fundamentally updated presentation of the concept of the protonmotive force, and a critical discussion on reporting data of mitochondrial respiration in terms of metabolic flows and fluxes.

Keywords: Mitochondrial respiratory control, coupling control, mitochondrial preparations, protonmotive force, chemiosmotic theory, oxidative phosphorylation, OXPHOS, efficiency, electron transfer, ET; proton leak, LEAK, residual oxygen consumption, ROX, State 2, State 3, State 4, normalization, flow, flux

---

Box 1:

In brief: Mitochondria and Bioblasts

- Does the public expect biologists to understand Darwin's theory of evolution?
- Do students expect that researchers of bioenergetics can explain Mitchell's theory of chemiosmotic energy transformation?

Mitochondria are the oxygen-consuming electrochemical generators which evolved from endosymbiotic bacteria (Margulis 1970; Lane 2005). They were described by Richard Altmann (1894) as 'bioblasts', which include not only the mitochondria as presently defined, but also symbiotic and free-living bacteria. The word 'mitochondria' (Greek mitos: thread; chondros: granule) was introduced by Carl Benda (1898).

Mitochondrial dysfunction is associated with a wide variety of genetic and degenerative diseases. Robust mitochondrial function is supported by physical exercise and caloric balance, and is central for sustained metabolic health throughout life. Therefore, a more consistent presentation of mitochondrial physiology will improve our understanding of the etiology of disease, the diagnostic repertoire of mitochondrial medicine, with a focus on protective medicine, lifestyle and healthy aging.

We now recognize mitochondria as dynamic organelles with a double membrane that are contained within eukaryotic cells. The mitochondrial inner membrane (mtIM) shows dynamic tubular to disk-shaped cristae that separate the mitochondrial matrix, *i.e.*, the negatively charged internal mitochondrial compartment, and the intermembrane space; the latter being positively charged and enclosed by the mitochondrial outer membrane (mtOM). The mtIM contains the non-bilayer phospholipid cardiolipin, which is not present in any other eukaryotic cellular membrane. Cardiolipin promotes the formation of respiratory supercomplexes, which are supramolecular assemblies based upon specific, though dynamic, interactions between

individual respiratory complexes (Greggio *et al.* 2017; Lenaz *et al.* 2017). Membrane fluidity is an important parameter influencing functional properties of proteins incorporated in the membranes (Waczulikova *et al.* 2007).

Mitochondria are the structural and functional elemental units of cell respiration. Cell respiration is the consumption of oxygen by electron transfer coupled to electrochemical proton translocation across the mtIM. In the process of oxidative phosphorylation (OXPHOS), the reduction of O_2 is electrochemically coupled to the transformation of energy in the form of adenosine triphosphate (ATP; Mitchell 1961, 2011). Mitochondria are the powerhouses of the cell which contain the machinery of the OXPHOS-pathways, including transmembrane respiratory complexes (*i.e.*, proton pumps with FMN, Fe-S and cytochrome *b*, *c*, aa_3 redox systems); alternative dehydrogenases and oxidases; the coenzyme ubiquinone (Q); F-ATPase or ATP synthase; the enzymes of the tricarboxylic acid cycle and the fatty acid oxidation enzymes; transporters of ions, metabolites and co-factors; and mitochondrial kinases related to energy transfer pathways. The mitochondrial proteome comprises over 1,200 proteins (Calvo *et al.* 2015; 2017), mostly encoded by nuclear DNA (nDNA), with a variety of functions, many of which are relatively well known (*e.g.* apoptosis-regulating proteins), while others are still under investigation, or need to be identified (*e.g.* alanine transporter).

There is a constant crosstalk between mitochondria and the other cellular components, maintaining cellular mitostasis through regulation at both the transcriptional and post-translational level, and through cell signalling including proteostatic (e.g. the ubiquitin-proteasome and autophagy-lysosome pathways) and genome stability modules throughout the cell cycle or even cell death, contributing to homeostatic regulation in response to varying energy demands and stress (Quiros *et al.* 2016). In addition to mitochondrial movement along the microtubules, mitochondrial morphology can change in response to energy requirements of the cell via processes known as fusion and fission, through which mitochondria communicate within a network, and in response to intracellular stress factors causing swelling and ultimately permeability transition.

Mitochondria typically maintain several copies of their own genome (hundred to thousands per cell; Cummins 1998), which is maternally inherited (White *et al.* 2008) and known as mitochondrial DNA (mtDNA). One exception to strictly maternal inheritance in animals is found in bivalves (Breton *et al.* 2007). mtDNA is 16.5 kB in length, contains 13 protein-coding genes for subunits of the transmembrane respiratory Complexes CI, CIII, CIV and F-ATPase, and also encodes 22 tRNAs and the mitochondrial 16S and 12S rRNA. Additional gene content is encoded in the mitochondrial genome, *e.g.* microRNAs, piRNA, smithRNAs, repeat associated RNA, and even additional proteins (Duarte *et al.* 2014; Lee *et al.* 2015; Cobb *et al.* 2016). The mitochondrial genome is both regulated and supplemented by nuclear-encoded mitochondrial targeted proteins.

Abbreviation: mt, as generally used in mtDNA. Mitochondrion is singular and mitochondria is plural.

'*For the physiologist, mitochondria afforded the first opportunity for an experimental approach to structure-function relationships, in particular those involved in active transport, vectorial metabolism, and metabolic control mechanisms on a subcellular level*' (Ernster and Schatz 1981).

1. Introduction

Mitochondria are the powerhouses of the cell with numerous physiological, molecular, and genetic functions (**Box 1**). Every study of mitochondrial function and disease is faced with **E**volution, **A**ge, **G**ender and sex, **L**ifestyle, and **E**nvironment (EAGLE) as essential background conditions intrinsic to the individual patient or subject, cohort, species, tissue and to some extent even cell line. As a large and highly coordinated group of laboratories and researchers, the

mission of the global MitoEAGLE Network is to generate the necessary scale, type, and quality of consistent data sets and conditions to address this intrinsic complexity. Harmonization of experimental protocols and implementation of a quality control and data management system are required to interrelate results gathered across a spectrum of studies and to generate a rigorously monitored database focused on mitochondrial respiratory function. In this way, researchers within the same and across different disciplines will be positioned to compare findings across traditions and generations to an agreed upon set of clearly defined and accepted international standards.

Reliability and comparability of quantitative results depend on the accuracy of measurements under strictly-defined conditions. A conceptual framework is required to warrant meaningful interpretation and comparability of experimental outcomes carried out by research groups at different institutes. With an emphasis on quality of research, collected data can be useful far beyond the specific question of a particular experiment. Enabling meta-analytic studies is the most economic way of providing robust answers to biological questions (Cooper *et al.* 2009). Vague or ambiguous jargon can lead to confusion and may relegate valuable signals to wasteful noise. For this reason, measured values must be expressed in standardized units for each parameter used to define mitochondrial respiratory function. Standardization of nomenclature and definition of technical terms are essential to improve the awareness of the intricate meaning of current and past scientific vocabulary, for documentation and integration into databases in general, and quantitative modelling in particular (Beard 2005). The focus on the protonmotive force, coupling states, and fluxes through metabolic pathways of aerobic energy transformation in mitochondrial preparations is a first step in the attempt to generate a harmonized and conceptually-oriented nomenclature in bioenergetics and mitochondrial physiology. The protonmotive force is a potential difference, Δp, and thus is not a force as defined in physics. Therefore, a detailed formal treatment is warranted of isomorphic forces and fluxes in bioenergetics. Coupling states of intact cells and respiratory control by fuel substrates and specific inhibitors of respiratory enzymes will be reviewed in subsequent communications.

2. Oxidative phosphorylation and coupling states in mitochondrial preparations

> '*Every professional group develops its own technical jargon for talking about matters of critical concern ... People who know a word can share that idea with other members of their group, and a shared vocabulary is part of the glue that holds people together and allows them to create a shared culture*' (Miller 1991).

Mitochondrial preparations are defined as either isolated mitochondria, or tissue and cellular preparations in which the barrier function of the plasma membrane is disrupted. The plasma membrane separates the cytosol, nucleus, and organelles (the intracellular compartment) from the environment of the cell. The plasma membrane consists of a lipid bilayer, embedded proteins, and attached organic molecules that collectively control the selective permeability of ions, organic molecules, and particles across the cell boundary. The intact plasma membrane, therefore, prevents the passage of many water-soluble mitochondrial substrates, such as succinate or adenosine diphosphate (ADP), that are required for the analysis of respiratory capacity at kinetically-saturating concentrations, thus limiting the scope of investigations into mitochondrial respiratory function in intact cells. The cholesterol content of the plasma membrane is high compared to mitochondrial membranes. Therefore, mild detergents, such as digitonin and saponin, can be applied to selectively permeabilize the plasma membrane by interaction with cholesterol and allow free exchange of cytosolic components with ions and organic molecules of the immediate cell environment, while maintaining the integrity and localization of organelles, cytoskeleton, and the nucleus. Application of optimum

concentrations of permeabilization agents (mild detergents or toxins) leads to the complete loss of cell viability, tested by nuclear staining and washout of cytosolic marker enzymes such as lactate dehydrogenase, while mitochondrial function remains intact. The respiration rate of isolated mitochondria remains unaltered after the addition of low concertations of digitonin or saponin. In addition to mechanical permeabilization during homogenization of tissue, peremeabilization agents may be applied to ensure permeabilization of all cells. Suspensions of cells permeabilized in the respiration chamber and crude tissue homogenates contain all components of the cell at highly diluted concentrations. All mitochondria are retained in chemically-permeabilized mitochondrial preparations and crude tissue homogenates. In the preparation of isolated mitochondria, the cells or tissues are homogenized, and the mitochondria are separated from other cell fractions and purified by differential centrifugation, entailing the loss of a fraction of mitochondria. Typical mitochondrial recovery ranges from 30% to 80%. Maximization of the purity of isolated mitochondria may compromise not only the mitochondrial yield but also the structural and functional integrity. Therefore, protocols for isolation of mitochondria need to be optimized according to the relevant questions addressed in a study. The term mitochondrial preparation does not include further fractionation of mitochondrial components, as well as submitochondrial particles.

2.1. Three coupling states of mitochondrial preparations and residual oxygen consumption

Respiratory capacities in coupling control states: To extend the classical nomenclature on mitochondrial coupling states (Section 2.3) by a concept-driven terminology that incorporates explicitly information on the nature of respiratory states, the terminology must be general and not restricted to any particular experimental protocol or mitochondrial preparation (Gnaiger 2009). We focus primarily on the conceptual 'why', along with clarification of the experimental 'how'. In the following section, the concept-driven terminology is explained and coupling states are defined. We define respiratory capacities, comparable to channel capacity in information theory (Schneider 2006), as the upper bound of the rate of respiration measured in defined coupling control states and electron transfer-pathway (ET-pathway) states.

To provide a diagnostic reference for respiratory capacities of core energy metabolism, the capacity of *oxidative phosphorylation*, OXPHOS, is measured at kinetically-saturating concentrations of ADP and inorganic phosphate, P_i. The *oxidative* ET-capacity reveals the limitation of OXPHOS-capacity mediated by the *phosphorylation*-pathway. The ET- and phosphorylation-pathways comprise coupled segments of the OXPHOS-system. ET-capacity is measured as noncoupled respiration by application of *external uncouplers*. The contribution of *intrinsically uncoupled* oxygen consumption is most easily studied in the absence of ADP, *i.e.*, by not stimulating phosphorylation, or by inhibition of the phosphorylation-pathway. The corresponding states are collectively classified as LEAK-states, when oxygen consumption compensates mainly for ion leaks including the proton leak (**Table 1**). Defined coupling states are induced by: (*1*) adding cation chelators such as EGTA, binding free Ca^{2+} and thus limiting cation cycling; (*2*) adding ADP and P_i; (*3*) inhibiting the phosphorylation-pathway; and (*4*) uncoupler titrations, while maintaining a defined ET-pathway state with constant fuel substrates and inhibitors of specific branches of the ET-pathway (**Fig. 1**).

Kinetic control: Coupling control states are established in the study of mitochondrial preparations to obtain reference values for various output variables. Physiological conditions *in vivo* deviate from these experimentally obtained states. Since kinetically-saturating concentrations, *e.g.* of ADP or oxygen, may not apply to physiological intracellular conditions, relevant information is obtained in studies of kinetic responses to conditions intermediate between the LEAK state at zero [ADP] and the OXPHOS-state at saturating [ADP], or of respiratory capacities in the range between kinetically-saturating [O_2] and anoxia (Gnaiger 2001).

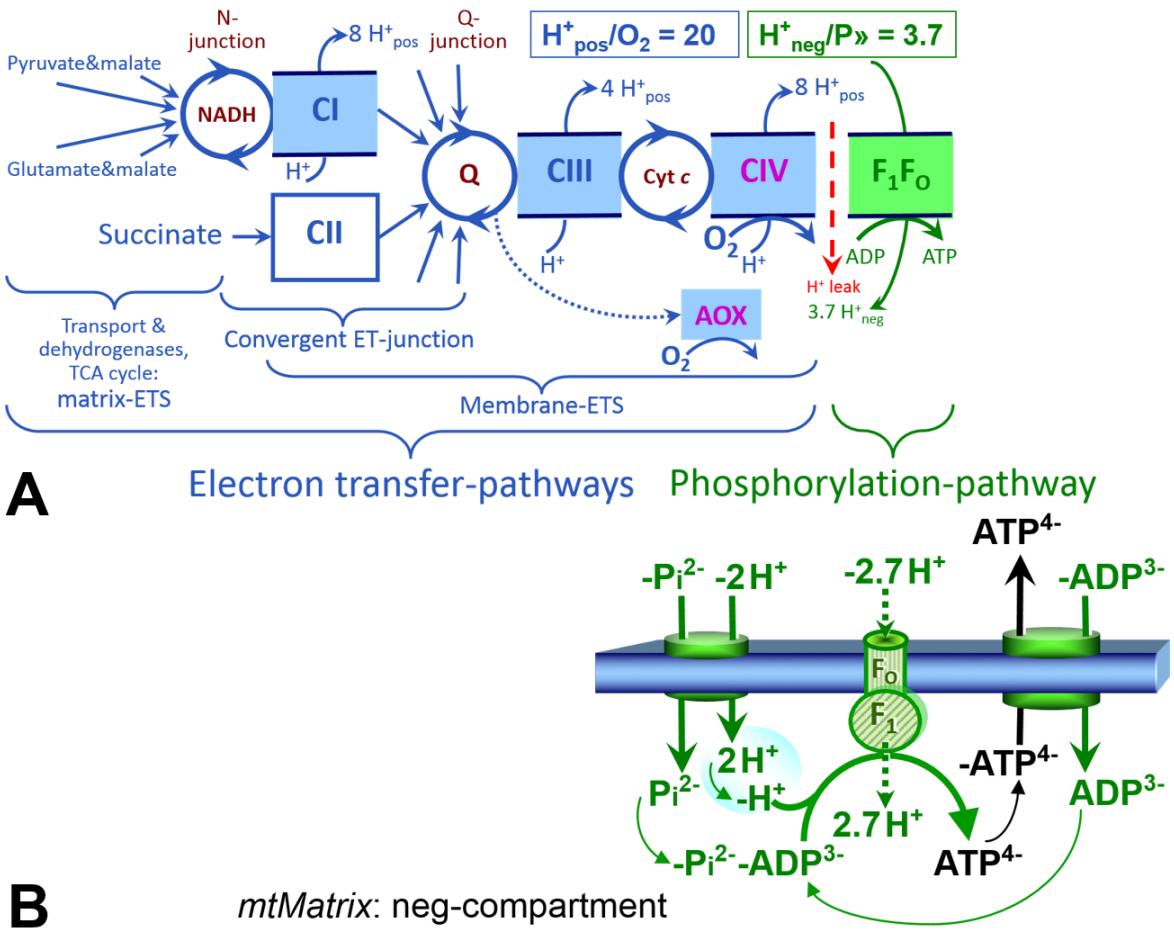

Fig. 1. The oxidative phosphorylation (OXPHOS) system. (A) The mitochondrial electron transfer system (ETS) is fuelled by diffusion and transport of substrates across the mtOM and mtIM and consists of the matrix-ETS and membrane-ETS. Electron transfer (ET) pathways are coupled to the phosphorylation-pathway. ET-pathways converge at the N-junction and Q-junction (additional arrows indicate electron entry into the Q-junction through electron transferring flavoprotein, glycerophosphate dehydrogenase, dihydro-orotate dehydrogenase, choline dehydrogenase, and sulfide-ubiquinone oxidoreductase). The dotted arrow indicates the branched pathway of oxygen consumption by alternative quinol oxidase (AOX). The H^+_{pos}/O_2 ratio is the outward proton flux from the matrix space to the positively (pos) charged compartment, divided by catabolic O_2 flux in the NADH-pathway. The H^+_{neg}/P» ratio is the inward proton flux from the inter-membrane space to the negatively (neg) charged matrix space, divided by the flux of phosphorylation of ADP to ATP (Eq. 1). Due to ion leaks and proton slip these are not fixed stoichiometries. (**B**) Phosphorylation-pathway catalyzed by the proton pump F_1F_O-ATPase, adenine nucleotide translocase, and inorganic phosphate transporter. The H^+_{neg}/P» stoichiometry is the sum of the coupling stoichiometry in the F-ATPase reaction (-2.7 H^+_{pos} from the positive intermembrane space, 2.7 H^+_{neg} to the matrix, *i.e.*, the negative compartment) and the proton balance in the translocation of ADP^{2-}, ATP^{3-} and P_i^{2-}. Modified from (A) Lemieux *et al*. (2017) and (B) Gnaiger (2014).

The steady-state: Mitochondria represent a thermodynamically open system in non-equilibrium states of biochemical energy transformation. State variables (protonmotive force; redox states) and metabolic *rates* (fluxes) are measured in defined mitochondrial respiratory *states*. Strictly, steady states can be obtained only in open systems, in which changes by *internal* transformations, *e.g.*, O_2 consumption, are instantaneously compensated for by *external* fluxes, *e.g.*, O_2 supply, such that oxygen concentration does not change in the system (Gnaiger 1993b).

Mitochondrial respiratory states monitored in closed systems satisfy the criteria of pseudo-steady states for limited periods of time, when changes in the system (concentrations of O_2, fuel substrates, ADP, P_i, H^+) do not exert significant effects on metabolic fluxes (respiration, phosphorylation). Such pseudo-steady states require respiratory media with sufficient buffering capacity and kinetically-saturating concentrations of substrates to be maintained, and thus depend on the kinetics of the processes under investigation.

Table 1. Coupling states and residual oxygen consumption in mitochondrial preparations in relation to respiration- and phosphorylation-rate, J_{kO_2} and $J_{P»}$, and protonmotive force, F_{mH+}. Coupling states are established at kinetically-saturating concentrations of fuel substrates and O_2.

State	J_{kO_2}	$J_{P»}$	F_{mH+}	Inducing factors	Limiting factors
LEAK	*L*; low, proton leak-dependent respiration	0	max.	Proton leak, slip, and cation cycling	$J_{P»}$ = 0: (*1*) without ADP, L_N; (*2*) max. ATP/ADP ratio, L_T; or (*3*) inhibition of the phosphorylation-pathway, L_{Omy}
OXPHOS	*P*; high, ADP-stimulated respiration	max.	high	Kinetically-saturating [ADP] and [P_i]	$J_{P»}$ by phosphorylation-pathway; or J_{kO_2} by ET-capacity
ET	*E*; max., noncoupled respiration	0	low	Optimal external uncoupler concentration for max. $J_{O_2,E}$	J_{kO_2} by ET-capacity
ROX	*Rox*; min., residual O_2 consumption	0	0	$J_{O_2,Rox}$ in non-ET-pathway oxidation reactions	Full inhibition of ET-pathway; or absence of fuel substrates

Specification of biochemical dose: Substrates, uncouplers, inhibitors, and other biochemical reagents are titrated to dissect mitochondrial function. Nominal concentrations of these substances are usually reported as initial amount of substance concentration [mol·L^{-1}] in the incubation medium. When aiming at the measurement of kinetically saturated processes such as OXPHOS-capacities, the concentrations for substrates can be chosen in light of the apparent equilibrium constant, K_m'. In the case of hyperbolic kinetics, only 80% of maximum respiratory capacity is obtained at a substrate concentration of four times the K_m', whereas substrate concentrations of 5, 9, 19 and 49 times the K_m' are theoretically required for reaching 83%, 90%, 95% or 98% of the maximal rate (Gnaiger 2001). Other reagents are chosen to inhibit or alter some process. The amount of these chemicals in an experimental incubation is selected to maximize effect, yet not lead to unacceptable off-target consequences that would adversely affect the data being sought. Specifying the amount of substance in an incubation as nominal concentration in the aqueous incubation medium can be ambiguous (Doskey *et al.* 2015), particularly when lipophilic substances (oligomycin; uncouplers, permeabilization agents) or cations (TPP^+; fluorescent dyes such as safranin, TMRM) are applied which accumulate in biological membranes or the mitochondrial matrix. For example, a dose of digitonin of 8 fmol·$cell^{-1}$ (10 µg·10^{-6} cells) is optimal for permeabilization of endothelial cells, and the concentration in the incubation medium has to be adjusted according to the cell density applied (Doerrier *et al.* 2018). Generally, dose/exposure can be specified per unit of biological

sample, *i.e.*, (nominal moles of xenobiotic)/(number of cells) [mol·cell^{-1}] or, as appropriate, per mass of biological sample [mol·kg^{-1}]. This approach to specification of dose/exposure provides a scalable parameter that can be used to design experiments, help interpret a wide variety of experimental results, and provide absolute information that allows researchers worldwide to make the most use of published data (Doskey *et al.* 2015).

Phosphorylation, P»: *Phosphorylation* in the context of OXPHOS is defined as phosphorylation of ADP by P_i to ATP. On the other hand, the term phosphorylation is used generally in many different contexts, *e.g.* protein phosphorylation. This justifies consideration of a symbol more discriminating and specific than P as used in the P/O ratio (phosphate to atomic oxygen ratio; O = 0.5 O_2), where P indicates phosphorylation of ADP to ATP or GDP to GTP. We propose the symbol P» for the endergonic (uphill) direction of phosphorylation ADP→ATP, and likewise the symbol P« for the corresponding exergonic (downhill) hydrolysis ATP→ADP (**Fig. 2**). P» refers mainly to electrontransfer phosphorylation but may also involve substrate-level phosphorylation as part of the tricarboxylic acid cycle (succinyl-CoA ligase) and phosphorylation of ADP catalyzed by phosphoenolpyruvate carboxykinase. Transphosphorylation is performed by adenylate kinase, creatine kinase, hexokinase and nucleoside diphosphate kinase. In isolated mammalian mitochondria ATP production catalyzed by adenylate kinase, 2 ADP ↔ ATP + AMP, proceeds without fuel substrates in the presence of ADP (Komlódi and Tretter 2017). Kinase cycles are involved in intracellular energy transfer and signal transduction for regulation of energy flux.

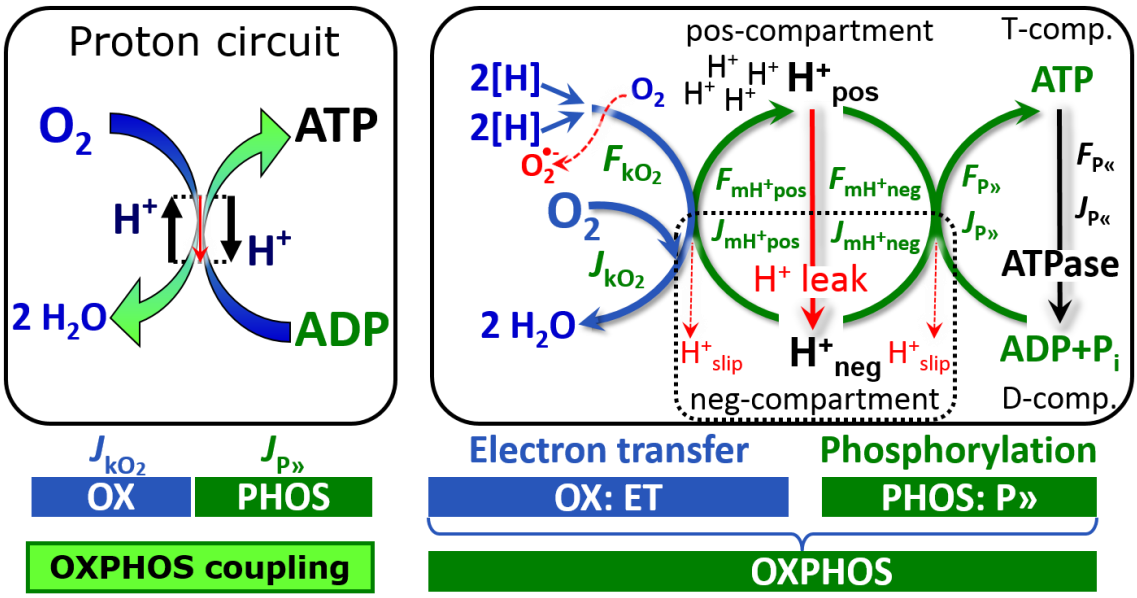

Fig. 2. The proton circuit and coupling in oxidative phosphorylation (OXPHOS). Oxygen flux, J_{kO_2}, through the catabolic ET-pathway, k, is coupled to flux through the phosphorylation-pathway of ADP to ATP, $J_{P»}$, by the proton pumps of the ET-pathway, driving the outward proton flux to the positive (pos) compartment, J_{mH^+pos}, and generating the output protonmotive force, F_{mH^+pos}. F-ATPase is coupled to inward proton current to the negative (neg) compartment, J_{mH^+neg}, to phosphorylate ADP+P_i to ATP, driven by the input protonmotive force, $F_{mH^+neg} = -F_{mH^+pos}$. 2[H] indicates the reduced hydrogen equivalents of fuel substrates that provide the chemical input force, F_{kO_2} [kJ/mol O_2], of the catabolic reaction k with oxygen (Gibbs energy of reaction per mole O_2 consumed in reaction k), typically in the range of -460 to -480 kJ/mol (1.2 V). The output force is given by the phosphorylation potential difference (ADP phosphorylated to ATP), $F_{P»}$, which varies *in vivo* ranging from about 48 to 62 kJ/mol under physiological conditions (Gnaiger 1993a). Fluxes, J_B, and forces, F_B, are expressed in either chemical units, [mol·s^{-1}·m^{-3}] and [J·mol^{-1}] respectively, or electrical units, [C·s^{-1}·m^{-3}] and

[J·C^{-1}] respectively. Fluxes are expressed per volume, V [m^3], of the system. The system defined by the boundaries (full black line) is not a black box, but is analysed as a compartmental system. The negative compartment (neg-compartment, enclosed by the dotted line) is the matrix space, separated by the mtIM from the positive compartment (pos-compartment). ADP+P_i and ATP are the substrate- and product-compartments (scalar ADP and ATP compartments, D-comp. and T-comp.), respectively. Chemical potentials of all substrates and products involved in the scalar reactions are measured in the pos-compartment for calculation of the scalar forces F_{kO_2} and $F_{P\text{»}} = -F_{P\text{«}}$. Proton turnover, $J_{\infty H^+}$, and ATP turnover, $J_{\infty P}$, proceed at steady-state and constant F_{mH^+}, when $J_{mH^+\infty} = J_{mH^+pos} = J_{mH^+neg}$, $F_{P\text{»}}$ is constant, and $J_{P\infty} = J_{P\text{»}} = J_{P\text{«}}$. Modified from Gnaiger (2014).

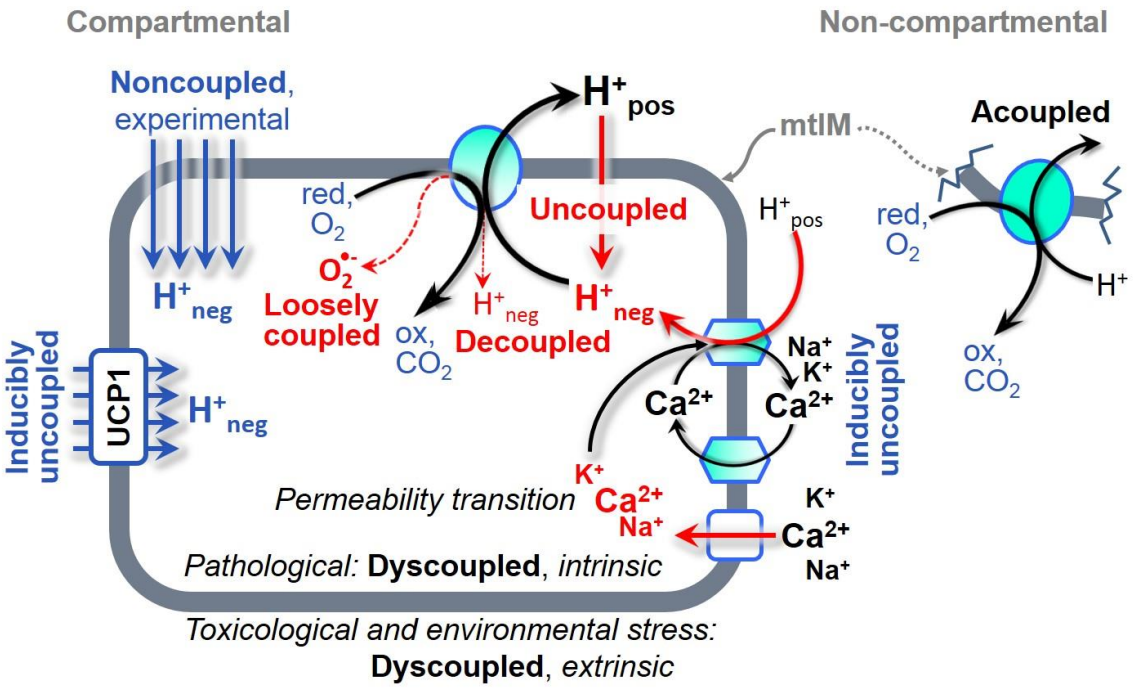

Fig 3. Mechanisms of respiratory uncoupling. An intact mitochondrial inner membrane, mtIM, is required for vectorial, compartmental coupling. 'Acoupled' respiration is the consequence of structural disruption with catalytic activity of non-compartmental mitochondrial fragments. Inducibly uncoupled (activation of UCP1) and experimentally noncoupled respiration (titration of protonophores) stimulate respiration to maximum oxygen flux of ET-capacity. Uncoupled, decoupled, and loosely coupled respiration are components of intrinsic LEAK respiration. Pathological dysfunction may affect all types of uncoupling, including permeability transition, causing intrinsically dyscoupled respiration. Similarly, toxicological and environmental stress factors can cause extrinsically dyscoupled respiration.

Uncoupling: Uncoupling is a general term comprising diverse mechanisms. Small differences of terms, *e.g.*, uncoupled *vs.* noncoupled, are easily overlooked, although they relate to different mechanisms of uncoupling (**Fig. 3**). An attempt at rigorous definition is required for clarification of concepts (**Table 2**).

1. Proton leak across the mtIM from the pos- to the neg-compartment (**Fig. 2**);
2. Cycling of other cations, strongly stimulated by permeability transition;
3. Proton slip in the proton pumps when protons are effectively not pumped (CI, CIII and CIV) or are not driving phosphorylation (F-ATPase);
4. Loss of compartmental integrity when electron transfer is acoupled;
5. Electron leak in the loosely coupled univalent reduction of oxygen (O_2; dioxygen) to superoxide anion radical ($O_2^{\bullet-}$).

LEAK-state (**Fig. 4**): The LEAK-state is defined as a state of mitochondrial respiration when O_2 flux mainly compensates for ion leaks in the absence of ATP synthesis, at kinetically-saturating concentrations of O_2 and respiratory fuel substrates. LEAK-respiration is measured to obtain an estimate of *intrinsic uncoupling* without addition of an experimental uncoupler: (*1*) in the absence of adenylates; (*2*) after depletion of ADP at a maximum ATP/ADP ratio; or (*3*) after inhibition of the phosphorylation-pathway by inhibitors of F-ATPase, such as oligomycin, or of adenine nucleotide translocase, such as carboxyatractyloside. It is important to consider adjustment of the nominal concentration of these inhibitors to the density of biological sample applied, to minimize or avoid inhibitory side-effects exerted on ET-capacity or even some dyscoupling.

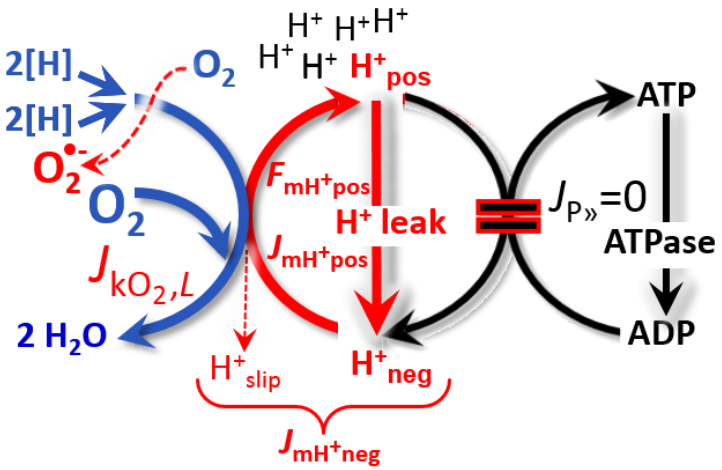

Fig. 4. LEAK-state: Phosphorylation is arrested, $J_{P»} = 0$, and catabolic oxygen flux, $J_{kO_2,L}$, is controlled mainly by the proton leak, $J_{mH^+neg,L}$, at maximum protonmotive force, F_{mH^+pos}. See also Fig. 2 and 3.

Table 2. Distinction of terms related to coupling and uncoupling (Fig. 3).

Term	Respiration	P»/O_2	Note
Acoupled		0	Electron transfer in mitochondrial fragments without vectorial proton translocation
Uncoupled	*L*	0	Non-phosphorylating intrinsic LEAK-respiration, without added protonophore
Uncoupled		0	Component of LEAK-respiration, uncoupled *sui generis*, ion diffusion across the mtIM
Decoupled		0	Component of LEAK-respiration, proton slip
Loosely coupled		0	Component of LEAK-respiration, lower coupling due to superoxide anion radical formation and bypass of proton pumps
Dyscoupled		0	Pathologically, toxicologically, environmentally increased uncoupling, mitochondrial dysfunction
Inducibly uncoupled	*E*	0	By UCP1 or cation (*e.g.* Ca^{2+}) cycling
Noncoupled	*E*	0	Non-phosphorylating respiration stimulated to maximum flux at optimum exogenous uncoupler concentration (**Fig. 6**)
Well-coupled	*P*	high	Phosphorylating respiration with an intrinsic LEAK component (**Fig. 5**)
Fully coupled	*P* – *L*	max.	OXPHOS-capacity corrected for LEAK-respiration (**Fig. 7**)

Proton leak and uncoupled respiration: Proton leak is a leak current of protons. The intrinsic proton leak is the *uncoupled* process in which protons diffuse across the mtIM in the dissipative direction of the downhill protonmotive force without coupling to phosphorylation (**Fig. 4**). The proton leak flux depends non-linearly on the protonmotive force (Garlid *et al.* 1989; Divakaruni and Brand 2011), is a property of the mtIM, and may be enhanced due to possible contaminations by free fatty acids. Inducible uncoupling mediated by uncoupling protein 1 (UCP1) is physiologically controlled, *e.g.*, in brown adipose tissue. UCP1 is a member of the mitochondrial carrier family which is involved in the translocation of protons across the mtIM (Klingenberg 2017). As a consequence of this effective short-circuit, the protonmotive force diminishes, resulting in stimulation of electron transfer to O_2 and heat dissipation without phosphorylation of ADP.

Cation cycling: There can be other cation contributors to leak current including calcium and probably magnesium. Calcium current is balanced by mitochondrial Na^+/Ca^{2+} exchange, which is balanced by Na^+/H^+ exchange or K^+/H^+ exchange. This is another effective uncoupling mechanism different from proton leak.

Proton slip and decoupled respiration: Proton slip is the *decoupled* process in which protons are only partially translocated by a proton pump of the ET-pathways and slip back to the original compartment. The proton leak is the dominant contributor to the overall leak current in mammalian mitochondria incubated under physiological conditions at 37 °C, whereas proton slip is increased at lower experimental temperature (Canton *et al.* 1995). Proton slip can also happen in association with the F-ATPase, in which case the proton slips downhill across the pump to the matrix without contributing to ATP synthesis. In each case, proton slip is a property of the proton pump and increases with the turnover rate of the pump.

Electron leak and loosely coupled respiration: Superoxide anion radical production by the ETS leads to a bypass of proton pumps and correspondingly lower P»/O_2 ratio, which depends on the actual site of electron leak and the scavenging of hydrogen peroxide by cytochrome *c*, whereby electrons may re-enter the ETS with proton translocation by CIV.

Loss of compartmental integrity and acoupled respiration: Electron transfer and O_2 consumption proceed without compartmental proton translocation in disrupted mitochondrial fragments. Such fragments form during mitochondrial isolation, and may not fully fuse to re-establish structurally intact mitochondria. Loss of mtIM integrity, therefore, is the cause of acoupled respiration, which is a nonvectorial dissipative process without control by the protonmotive force.

Dyscoupled respiration: Mitochondrial injuries may lead to *dyscoupling* as a pathological or toxicological cause of *uncoupled* respiration. Dyscoupling may involve any type of uncoupling mechanism, *e.g.*, opening the permeability transition pore. Dyscoupled respiration is distinguished from the experimentally induced *noncoupled* respiration in the ET-state (**Fig. 3**).

OXPHOS-state (**Fig. 5**): The OXPHOS-state is defined as the respiratory state with kinetically-saturating concentrations of O_2, respiratory and phosphorylation substrates, and absence of exogenous uncoupler, which provides an

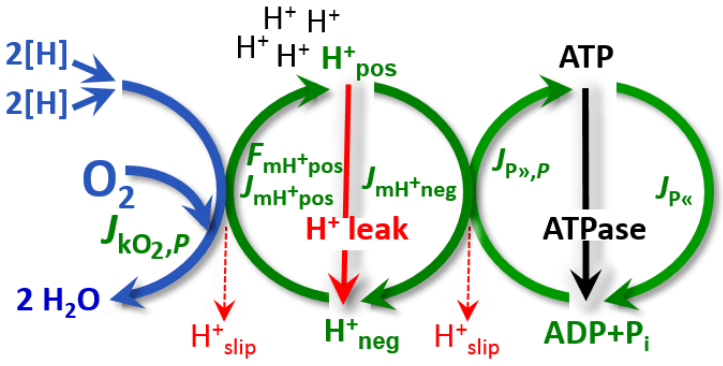

Fig. 5. OXPHOS-state: Phosphorylation, $J_{P»}$, is stimulated by kinetically-saturating [ADP] and inorganic phosphate, [P_i], and is supported by a high protonmotive force, F_{mH^+pos}. O_2 flux, $J_{kO_2,P}$, is well-coupled at a P»/O_2 ratio of $J_{P»,P}/J_{O_2,P}$. See also Fig. 2.

estimate of the maximal respiratory capacity in the OXPHOS-state for any given ET-pathway state. Respiratory capacities at kinetically-saturating substrate concentrations provide reference values or upper limits of performance, aiming at the generation of data sets for comparative purposes. Physiological activities and effects of substrate kinetics can be evaluated relative to the OXPHOS-capacity.

As discussed previously, 0.2 mM ADP does not fully saturate flux in isolated mitochondria (Gnaiger 2001; Puchowicz *et al.* 2004); greater ADP concentration is required, particularly in permeabilized muscle fibres and cardiomyocytes, to overcome limitations by intracellular diffusion and by the reduced conductance of the mtOM (Jepihhina *et al.* 2011, Illaste *et al.* 2012, Simson *et al*. 2016), either through interaction with tubulin (Rostovtseva *et al.* 2008) or other intracellular structures (Birkedal *et al*. 2014). In permeabilized muscle fibre bundles of high respiratory capacity, the apparent K_m for ADP increases up to 0.5 mM (Saks *et al.* 1998), consistent with experimental evidence that >90% saturation is reached only at >5 mM ADP (Pesta and Gnaiger 2012). Similar ADP concentrations are also required for accurate determination of OXPHOS-capacity in human clinical cancer samples and permeabilized cells (Klepinin *et al.* 2016; Koit *et al.* 2017). Whereas 2.5 to 5 mM ADP is sufficient to obtain the actual OXPHOS-capacity in many types of permeabilized tissue and cell preparations, experimental validation is required in each specific case.

Electron transfer-state (**Fig. 6**): The ET-state is defined as the *noncoupled* state with kinetically-saturating concentrations of O_2, respiratory substrate and optimum *exogenous* uncoupler concentration for maximum O_2 flux, as an estimate of ET-capacity. Inhibition of respiration is observed at higher than optimum uncoupler concentrations. As a consequence of the nearly collapsed protonmotive force, the driving force is insufficient for phosphorylation, and $J_{P\text{»}} = 0$.

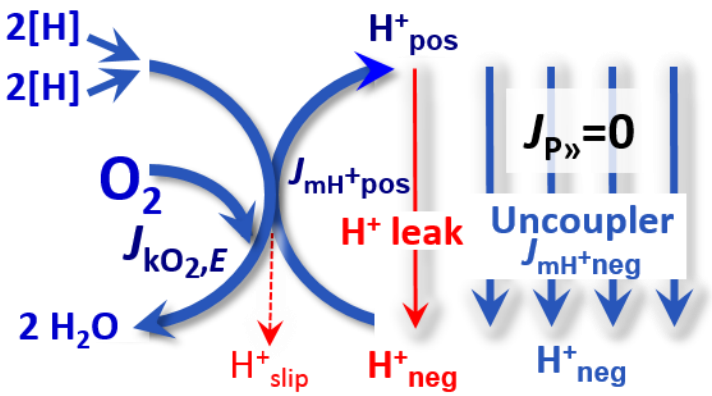

Fig. 6. ET-state: Noncoupled respiration, $J_{kO2,E}$, is maximum at optimum exogenous uncoupler concentration and phosphorylation is zero, $J_{P\text{»}} = 0$. See also Fig. 2.

Besides the three fundamental coupling states of mitochondrial preparations, the following respiratory state also is relevant to assess respiratory function:

ROX state and *Rox*: The rate of residual oxygen consumption, *Rox*, is defined as O_2 consumption due to oxidative side reactions remaining after inhibition of ET, *e.g.*, with rotenone, malonic acid and antimycin A. Cyanide and azide not only inhibit CIV but several peroxidases which should be involved in *Rox*. ROX is not a coupling state. *Rox* represents a baseline that is used to correct mitochondrial respiration in defined coupling states. *Rox* is not necessarily equivalent to non-mitochondrial respiration, considering oxygen-consuming reactions in mitochondria not related to ET, such as oxygen consumption in reactions catalyzed by monoamine oxidases (type A and B), monooxygenases (cytochrome P450 monooxygenases), dioxygenase (sulfur dioxygenase and trimethyllysine dioxygenase), several hydoxylases, and more. Mitochondrial preparations, especially those obtained from liver, may be contaminated by peroxisomes. This fact makes the exact determination of mitochondrial oxygen consumption and mitochondria-associated generation of reactive oxygen species complicated (Schönfeld *et al.* 2009). The dependence of ROX-linked oxygen consumption

needs to be studied in detail with respect to non-ET enzyme activities, availability of specific substrates, oxygen concentration, and electron leakage leading to the formation of reactive oxygen species.

2.2. Coupling states and respiratory rates

As an improvement of previous terminologies, we distinguish metabolic *pathways* from metabolic *states* and the corresponding metabolic *rates*; for example: ET-pathways (**Fig. 7**), ET-state (**Fig. 6**), and ET-capacity, *E*, respectively (**Table 1**). The protonmotive force is *high* in the OXPHOS-state when it drives phosphorylation, *maximum* in the LEAK-state of coupled mitochondria, driven by LEAK-respiration at a minimum back flux of cations to the matrix side, and *very low* in the ET-state when uncouplers short-circuit the proton cycle (**Table 1**).

The three coupling states, ET, LEAK and OXPHOS, are shown schematically with the corresponding respiratory rates, abbreviated as *E*, *L* and *P*, respectively (**Fig. 7**).

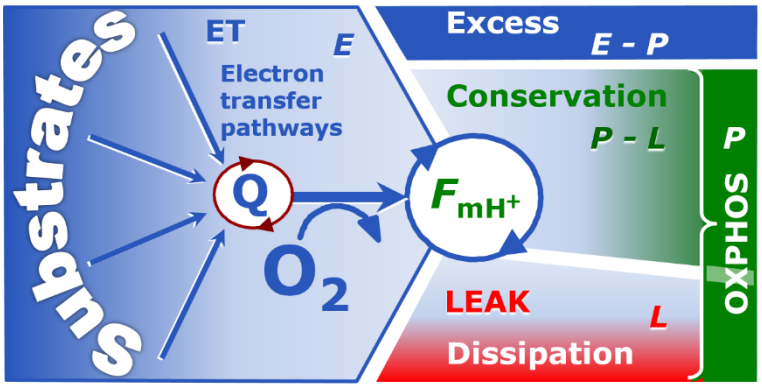

Fig. 7. Four-compartment model of oxidative phosphorylation. Respiratory states (ET, OXPHOS, LEAK) and corresponding rates (*E*, *P*, *L*) are connected by the protonmotive force, F_{mH^+}. Electron transfer-capacity, *E*, is partitioned into (*1*) dissipative LEAK-respiration, *L*, when the Gibbs energy change of catabolic O_2 consumption is irreversibly lost, (*2*) net OXPHOS-capacity, *P-L*, with partial conservation of the capacity to perform work, and (*3*) the excess capacity, *E-P*. Modified from Gnaiger (2014).

E may exceed or be equal to *P*. *E* > *P* is observed in many types of mitochondria, varying between species, tissues and cell types (Gnaiger 2009). *E-P* is the excess ET-capacity pushing the phosphorylation-flux (**Fig. 1B**) to the limit of its *capacity of utilizing* the protonmotive force. In addition, the magnitude of *E-P* depends on the tightness of coupling or degree of uncoupling, since an increase of *L* causes *P* to increase towards the limit of *E*. The *excess E-P* capacity, *E-P*, therefore, provides a sensitive diagnostic indicator of specific injuries of the phosphorylation-pathway, under conditions when *E* remains constant but *P* declines relative to controls (**Fig. 7**). Substrate cocktails supporting simultaneous convergent electron transfer to the Q-junction for reconstitution of tricarboxylic acid cycle (TCA cycle or Krebs cycle) function establish pathway control states with high ET-capacity, and consequently increase the sensitivity of the *E-P* assay.

E cannot theoretically be lower than *P*. *E* < *P* must be discounted as an artefact, which may be caused experimentally by: (*1*) loss of oxidative capacity during the time course of the respirometric assay, since *E* is measured subsequently to *P*; (*2*) using insuffient uncoupler concentrations; (*3*) using high uncoupler concentrations which inhibit ET (Gnaiger 2008); (*4*) high oligomycin concentrations applied for measurement of *L* before titrations of uncoupler, when oligomycin exerts an inhibitory effect on *E*. On the other hand, the excess ET-capacity is overestimated if non-saturating [ADP] or [P_i] are used. See State 3 in the next section.

P»/O_2 ratio: The P»/O_2 ratio (P»/4 e^-) is two times the 'P/O' ratio (P»/2 e^-) of classical bioenergetics. P»/O_2 is a generalized symbol, independent of measurement of phosphorylation

662 by determination of P_i consumption (P_i/O_2 flux ratio), ADP depletion (ADP/O_2 flux ratio), or
663 ATP production (ATP/O_2 flux ratio).
664 The mechanistic P»/O_2 ratio, which may be referred to also as P»/O_2 stoichiometry, is
665 calculated from the proton-to-oxygen and proton-to-phosphorylation coupling stoichiometries
666 (**Fig. 1A**),
667

668 $$P\text{»}/O_2 = \frac{H^+_{pos}/O_2}{H^+_{neg}/P\text{»}} \quad (1)$$

669
670 The H^+_{pos}/O_2 *coupling stoichiometry* (referring to the full 4 electron reduction of O_2) depends
671 on the ET-pathway control state which defines the relative involvement of the three coupling
672 sites (CI, CIII and CIV) in the catabolic pathway of electrons to O_2. This varies with: (*1*) a
673 bypass of CI by single or multiple electron input into the Q-junction; and (*2*) a bypass of CIV
674 by involvement of AOX. H^+_{pos}/O_2 is 12 in the ET-pathways involving CIII and CIV as proton
675 pumps, increasing to 20 for the NADH-pathway (**Fig. 1A**), but a general consensus on H^+_{pos}/O_2
676 stoichiometries remains to be reached (Hinkle 2005; Wikström and Hummer 2012; Sazanov
677 2015). The H^+_{neg}/P» coupling stoichiometry (3.7; **Fig. 1A**) is the sum of 2.7 H^+_{neg} required by
678 the F-ATPase of vertebrate and most invertebrate species (Watt *et al.* 2010) and the proton
679 balance in the translocation of ADP, ATP and P_i (**Fig. 1B**). Taken together, the mechanistic
680 P»/O_2 ratio is calculated at 5.4 and 3.3 for NADH- and succinate-linked respiration, respectively
681 (Eq. 1). The corresponding classical P»/O ratios (referring to the 2 electron reduction of 0.5 O_2)
682 are 2.7 and 1.6 (Watt *et al.* 2010), in direct agreement with the measured P»/O ratio for succinate
683 of 1.58 ± 0.02 (Gnaiger *et al.* 2000).
684 The effective P»/O_2 flux ratio ($Y_{P\text{»}/O_2} = J_{P\text{»}}/J_{kO_2}$) is diminished relative to the mechanistic
685 P»/O_2 ratio by intrinsic and extrinsic uncoupling and dyscoupling (**Fig. 3**). Such generalized
686 uncoupling is different from switching to mitochondrial pathways that involve fewer than three
687 proton pumps (‘coupling sites’: Complexes CI, CIII and CIV), bypassing CI through multiple
688 electron entries into the Q-junction, or CIII and CIV through AOX (**Fig. 1**). Reprogramming of
689 mitochondrial pathways may be considered as a switch of gears (changing the stoichiometry)
690 rather than uncoupling (loosening the stoichiometry). In addition, $Y_{P\text{»}/O_2}$ depends on several
691 experimental conditions of flux control, increasing as a hyperbolic function of [ADP] to a
692 maximum value (Gnaiger 2001).
693 The net OXPHOS-capacity is calculated by subtracting *L* from *P* (**Fig. 7**). Then the net
694 P»/O_2 equals P»/(*P*-*L*), wherein the dissipative LEAK component in the OXPHOS-state may
695 be overestimated. This can be avoided by measuring LEAK-respiration in a state when the
696 protonmotive force is adjusted to its slightly lower value in the OXPHOS-state, *e.g.*, by titration
697 of an ET inhibitor (Divakaruni and Brand 2011). Any turnover-dependent components of
698 proton leak and slip, however, are underestimated under these conditions (Garlid *et al.* 1993).
699 In general, it is inappropriate to use the term *ATP production* or *ATP turnover* for the difference
700 of oxygen consumption measured in states *P* and *L*. The difference *P*-*L* is the upper limit of the
701 part of OXPHOS-capacity that is freely available for ATP production (corrected for LEAK-
702 respiration) and is fully coupled to phosphorylation with a maximum mechanistic stoichiometry
703 (**Fig. 7**).
704 **Control and regulation:** The terms metabolic *control* and *regulation* are frequently used
705 synonymously, but are distinguished in metabolic control analysis: ‘We could understand the
706 regulation as the mechanism that occurs when a system maintains some variable constant over
707 time, in spite of fluctuations in external conditions (homeostasis of the internal state). On the
708 other hand, metabolic control is the power to change the state of the metabolism in response to
709 an external signal’ (Fell 1997). Respiratory control may be induced by experimental control
710 signals that *exert* an influence on: (*1*) ATP demand and ADP phosphorylation-rate; (*2*) fuel
711 substrate composition, pathway competition; (*3*) available amounts of substrates and oxygen,

e.g., starvation and hypoxia; (*3*) the protonmotive force, redox states, flux-force relationships, coupling and efficiency; (*4*) Ca^{2+} and other ions including H^{+}; (*5*) inhibitors, *e.g.*, nitric oxide or intermediary metabolites, such as oxaloacetate; (*6*) signalling pathways and regulatory proteins, *e.g.* insulin resistance, transcription factor HIF-1 or inhibitory factor 1. *Mechanisms* of respiratory control and regulation include adjustments of: (*1*) enzyme activities by allosteric mechanisms and phosphorylation; (*2*) enzyme content, concentrations of cofactors and conserved moieties (such as adenylates, nicotinamide adenine dinucleotide [NAD^{+}/NADH], coenzyme Q, cytochrome *c*); (*3*) metabolic channeling by supercomplexes; and *(4)* mitochondrial density (enzyme concentrations and membrane area) and morphology (cristae folding, fission and fusion). (*5*) Mitochondria are targeted directly by hormones, thereby affecting their energy metabolism (Lee *et al.* 2013; Gerö and Szabo 2016; Price and Dai 2016; Moreno *et al.* 2017). Evolutionary or acquired differences in the genetic and epigenetic basis of mitochondrial function (or dysfunction) between subjects and gene therapy; age; gender, biological sex, and hormone concentrations; life style including exercise and nutrition; and environmental issues including thermal, atmospheric, toxicological and pharmacological factors, exert an influence on all control mechanisms listed above. For reviews, see Brown 1992; Gnaiger 1993a, 2009; 2014; Paradies *et al.* 2014; Morrow *et al*. 2017.

Respiratory control and response: Lack of control by a metabolic pathway, *e.g.* phosphorylation-pathway, does mean that there will be no response to a variable activating it, *e.g.* [ADP]. However, the reverse is not true as the absence of a response to [ADP] does not exclude the phosphorylation-pathway from having some degree of control. The degree of control of a component of the OXPHOS-pathway on an output variable, such as oxygen flux, will in general be different from the degree of control on other outputs, such as phosphorylation-flux or proton leak flux. Therefore, it is necessary to be specific as to which input and output are under consideration (Fell 1997).

Respiratory coupling control: Respiratory control refers to the ability of mitochondria to adjust oxygen consumption in response to external control signals by engaging various mechanisms of control and regulation. Respiratory control is monitored in a mitochondrial preparation under conditions defined as respiratory states. When phosphorylation of ADP to ATP is stimulated or depressed, an increase or decrease is observed in electron flux linked to oxygen consumption in respiratory coupling states of intact mitochondria (‘controlled states’ in the classical terminology of bioenergetics). Alternatively, coupling of electron transfer with phosphorylation is disengaged by disruption of the integrity of the mtIM or by uncouplers, functioning like a clutch in a mechanical system. The corresponding coupling control state is characterized by high levels of oxygen consumption without control by phosphorylation (‘uncontrolled state’).

ET-pathway control states are obtained in mitochondrial preparations by depletion of endogenous substrates and addition to the mitochondrial respiration medium of fuel substrates (CHNO; 2[H]) and specific inhibitors, activating selected mitochondrial catabolic pathways, k (**Fig. 1 and 2**). Coupling control states and pathway control states are complementary, since mitochondrial preparations depend on an exogenous supply of pathway-specific fuel substrates and oxygen (Gnaiger 2014).

2.3. Classical terminology for isolated mitochondria

> *‘When a code is familiar enough, it ceases appearing like a code; one forgets that there is a decoding mechanism. The message is identical with its meaning’* (Hofstadter 1979).

Chance and Williams (1955; 1956) introduced five classical states of mitochondrial respiration and cytochrome redox states. **Table 3** shows a protocol with isolated mitochondria in a closed respirometric chamber, defining a sequence of respiratory states. States and rates are not specifically distinguished in this nomenclature.

Table 3. Metabolic states of mitochondria (Chance and Williams, 1956; Table V).

State	[O_2]	ADP level	Substrate Level	Respiration rate	Rate-limiting substance
1	>0	low	Low	slow	ADP
2	>0	high	~0	slow	substrate
3	>0	high	High	fast	respiratory chain
4	>0	low	High	slow	ADP
5	0	high	High	0	oxygen

State 1 is obtained after addition of isolated mitochondria to air-saturated isoosmotic/isotonic respiration medium containing inorganic phosphate, but no fuel substrates and no adenylates, *i.e.*, AMP, ADP, ATP.

State 2 is induced by addition of a 'high' concentration of ADP (typically 100 to 300 µM), which stimulates respiration transiently on the basis of endogenous fuel substrates and phosphorylates only a small portion of the added ADP. State 2 is then obtained at a low respiratory activity limited by exhausted endogenous fuel substrate availability (**Table 3**). If addition of specific inhibitors of respiratory complexes, such as rotenone, does not cause a further decline of oxygen consumption, State 2 is equivalent to the state of residual oxygen consumption, ROX (See below.). If inhibition is observed, undefined endogenous fuel substrates are a confounding factor of pathway control, contributing to the effect of subsequently externally added substrates and inhibitors. In contrast to the original protocol, an alternative sequence of titration steps is frequently applied, in which the alternative 'State 2' has an entirely different meaning, when this second state is induced by addition of fuel substrate without ADP (LEAK-state; in contrast to State 2 defined in **Table 1** as a ROX state), followed by addition of ADP.

State 3 is the state stimulated by addition of fuel substrates while the ADP concentration is still high (**Table 3**) and supports coupled energy transformation through oxidative phosphorylation. 'High ADP' is a concentration of ADP specifically selected to allow the measurement of State 3 to State 4 transitions of isolated mitochondria in a closed respirometric chamber. Repeated ADP titration re-establishes State 3 at 'high ADP'. Starting at oxygen concentrations near air-saturation (ca. 200 µM O_2 at sea level and 37 °C), the total ADP concentration added must be low enough (typically 100 to 300 µM) to allow phosphorylation to ATP at a coupled rate of oxygen consumption that does not lead to oxygen depletion during the transition to State 4. In contrast, kinetically-saturating ADP concentrations usually are an order of magnitude higher than 'high ADP', *e.g.* 2.5 mM in isolated mitochondria. The abbreviation State 3u is occasionally used in bioenergetics, to indicate the state of respiration after titration of an uncoupler, without sufficient emphasis on the fundamental difference between OXPHOS-capacity (*well-coupled* with an *endogenous* uncoupled component) and ET-capacity (*noncoupled*).

State 4 is a LEAK-state that is obtained only if the mitochondrial preparation is intact and well-coupled. Depletion of ADP by phosphorylation to ATP leads to a decline in the rate of oxygen consumption in the transition from State 3 to State 4. Under these conditions of State 4, a maximum protonmotive force and high ATP/ADP ratio are maintained. For calculation of P»/O_2 ratios the gradual decline of $Y_{P»/O_2}$ towards diminishing [ADP] at State 4 must be taken into account (Gnaiger 2001). State 4 respiration, L_T (**Table 1**), reflects intrinsic proton leak and intrinsic ATP hydrolysis activity. Oxygen consumption in State 4 is an overestimation of LEAK-respiration if the contaminating ATP hydrolysis activity recycles some ATP to ADP, $J_{P«}$, which stimulates respiration coupled to phosphorylation, $J_{P»} > 0$. This can be tested by inhibition of the phosphorylation-pathway using oligomycin, ensuring that $J_{P»} = 0$ (State 4o).

Alternatively, sequential ADP titrations re-establish State 3, followed by State 3 to State 4 transitions while sufficient oxygen is available. However, anoxia may be reached before exhaustion of ADP (State 5).

State 5 is the state after exhaustion of oxygen in a closed respirometric chamber. Diffusion of oxygen from the surroundings into the aqueous solution may be a confounding factor preventing complete anoxia (Gnaiger 2001). Chance and Williams (1955) provide an alternative definition of State 5, which gives it the different meaning of ROX versus anoxia: 'State 5 may be obtained by antimycin A treatment or by anaerobiosis'.

In **Table 3**, only States 3 and 4 (and 'State 2' in the alternative protocol without ADP; not included in the table) are coupling control states, with the restriction that O_2 flux in State 3 may be limited kinetically by non-saturating ADP concentrations (**Table 1**).

3. The protonmotive force, proton flux, and respiratory control

3.1. Electric and chemical partial forces expressed in various units

The protonmotive force across the mtIM, Δp (Mitchell 1961; Mitchell and Moyle 1967), is a characteristic of respiratory states (**Table 1**). Δp was introduced most elegantly in the *Grey Book 1966* (Mitchell 2011),

$$\Delta p = \Delta\Psi + \Delta\mu_{H^+}\cdot F^{-1} \quad (2)$$

Δp consists of two partial isomorphic forces: (*1*) The electric part, $\Delta\Psi$, is the electric potential difference, which is not specific for H^+ and can, therefore, be measured by the distribution of any permeable cation equilibrating between the positive and negative compartment (**Fig. 2**). (*2*) The chemical part contains the chemical potential difference in H^+, $\Delta\mu_{H^+}$, which is proportional to the pH difference, ΔpH (**Box 2**).

Protonmotive means that there is a potential for the movement of protons, and *force* is a measure of the potential for motion. Motion is relative and not absolute (Principle of Galilean Relativity); likewise there is no absolute potential, but isomorphic forces are potential differences, $\Delta\Psi$ and $\Delta\mu_{H^+}$ (**Table 4**). F is the Faraday constant (**Table 5**). According to its definition in physics, a potential difference and as such the *protonmotive force* is not a force *per se* (IUPAC: Cohen *et al.* 2008). Forces as defined in physics, $\boldsymbol{F}$ [$J\cdot m^{-2}$ = N], describe the interaction between particles as vectors with direction in space, that cause a change in the motion (acceleration) of the particles. The fundamental forces are the gravitational, electroweak (combining electromagnetic and weak nuclear) and strong nuclear forces. In contrast, the non-fundamental forces are distinguished as isomorphic *motive forces*, F_{tr}, in a variety of transformations, tr. These forces are frequently not vectors (**Box 3**) and are expressed in various *motive units*, MU [$J\cdot MU^{-1}$], depending on the energy transformation under study. This is the case for the protonmotive force, whereby the proton is the *motive entity*, which can be expressed in a variety of formats with different MU. Consistency of terms and symbols can be achieved with reference to isomorphic motive forces, F_{tr}, which express explicitely the meaning of the terms in Eq.(2) and show their connection (**Table 4**).

The electric and chemical components of the protonmotive force are added (motive = electric + chemical; Eq. 2). Since a physical quantity is the product of a numerical value and a unit, this is possible only when expressing the partial forces in a common format with identical units (**Box 2**). Among the ultimate unifying principles in physics is the concept of the particle. The protonmotive force can be expressed per particle (per proton molecule), in which case the MU for the proton is a pure number [x], and the unit of the *molecular force* is [$J\cdot x^{-1}$]. When the number of particles or molecules, N [x], are divided by the Avogadro constant, N_A [$x\cdot mol^{-1}$], the *molecular motive unit* [x] is converted to the *molar motive unit* mole [mol], whereas

multiplication of N by ze [C·x^{-1}] yields the *electrical motive unit* coulomb [C] (**Fig. 8**). When the protonmotive force is expressed in the electrical MU-format as a voltage (electrochemical potential difference; Eq. 2), the MU is the coulomb, and the unit of the *electrical force* is [J·C^{-1} ≡ V]. The molar MU-format of Eq.(2) is known as the chemiosmotic potential difference, where the MU is the mole, and the unit of the *molar force* is [J·mol^{-1}].

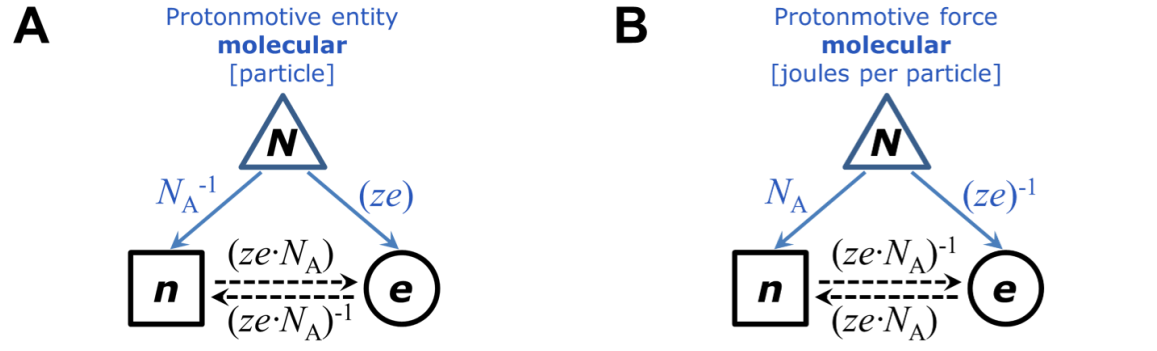

N to ***n***:	$J_{N\mathrm{mH^+}} \cdot N_A^{-1}$	$= J_{n\mathrm{mH^+}}$	[mol·s^{-1}·m^{-3}]	$F_{N\mathrm{mH^+}} \cdot N_A$	$= F_{n\mathrm{mH^+}}$	[J·mol^{-1}]
N to ***e***:	$J_{N\mathrm{mH^+}} \cdot (ze)$	$= J_{e\mathrm{mH^+}}$	[C·s^{-1}·m^{-3}]	$F_{N\mathrm{mH^+}} \cdot (ze)^{-1}$	$= F_{e\mathrm{mH^+}}$	[J·C^{-1}]
n to ***e***:	$J_{n\mathrm{mH^+}} \cdot (ze \cdot N_A)$	$= J_{e\mathrm{mH^+}}$	[C·s^{-1}·m^{-3}]	$F_{n\mathrm{mH^+}} \cdot (ze \cdot N_A)^{-1}$	$= F_{e\mathrm{mH^+}}$	[J·C^{-1}]

Fig. 8. Molecular, molar and electrical (*N*, *n*, *e*) formats and units of the protonmotive entity (A) and protonmotive force (B). Avogadro constant, N_A: molecules H^+ per mol H^+ [x·mol^{-1}]; charge number, z = 1: charges per H^+ [x·x^{-1}]; elementary charge, e: coulombs per electron [C·x^{-1}] (**Table 5**).

Unfortunately, the dimensionless unit [x] is not explicitely considered by IUPAC (Mohr and Philipps 2015). This causes confusion, since then the unit [J] (per system or per molecule) would indicate either an extensive quantity (energy per system [J]) or intensive quantity (force, energy per motive molecule [J·x^{-1}]) (**Box 2**). Even though the charge number z equals 1 for the proton, z should be written explicitely in Eq.(2) for physical consistency ($zF = ze \cdot N_A$; **Table 5**): The ratio of electrons per proton molecule (z=1) is multiplied by the elementary charge (e, ratio of coulombs per electron), which yields the ratio of coulombs per proton molecule [C·x^{-1}]. This is multiplied with N_A (the ratio of proton molecules per mole protons [x·mol^{-1}]), thus obtaining for $ze \cdot N_A$ the ratio of coulombs per mole protons [C·mol^{-1}] (**Fig. 8**).

The protonmotive force, $F_{\mathrm{mH^+}}$ [J·MU^{-1}], is conjugated to the transmembrane proton flux, $J_{\mathrm{mH^+}}$ [MU·s^{-1}·m^{-3}]. Conjugated quantities are linked by the same MU; in other words, they are expressed in the same MU-format. When different MU-formats are used, the format (***N***, ***n***, ***e***) is shown as a subscript ($F_{N\mathrm{mH^+}}$, $F_{n\mathrm{mH^+}}$, $F_{e\mathrm{mH^+}}$; **Fig. 8**). Further formats are theoretically possible, *e.g.*, mass (MU=kg) or energy with further specification (MU=J).

The electric partial force (el) is indicated by a subscript: F_{el}. Correspondingly, the chemical partial force of diffusion, d, is indicated by a subscript: $F_{\mathrm{dH^+}}$, with focus on the particle separate from the charge (**Table 4**). The total motive force (motive = electric + chemical) is distinguished from the partial components by subscript m, $F_{\mathrm{mH^+}}$. Reading this symbol backwards, starting with the proton, it can be seen as pmf, or the subscript m (motive) can be remembered by the name of Mitchell.

The compartmental direction of movement *into the positive compartment* is shown by subscript 'pos' for the force and flux: $F_{\mathrm{mH^+pos}}$ and $J_{\mathrm{mH^+pos}}$ (**Fig. 2**). The sign of the force is positive, when Gibbs energy is conserved in proton pumping. When the direction of flux is defined as movement into the negative compartment, $J_{\mathrm{mH^+neg}}$, the force, $F_{\mathrm{mH^+neg}}$, has a negative sign in the dissipative direction (**Box 4**).

Box 2: The partial protonmotive forces and conversion between motive units

The separation of partial isomorphic (electric and chemical) forces as the components of the protonmotive force (**Table 4**) must be clearly distinguished from the different MU-formats.

Protonmotive force, three MU-formats; z=1 (**Fig. 8B**)

N	Molecular format:	$F_{N\mathrm{mH^+}}$	$=$	$F_{\boldsymbol{n}\mathrm{mH^+}} \cdot N_\mathrm{A}^{-1}$	$=$ $F_{\boldsymbol{e}\mathrm{mH^+}} \cdot (ze)$	$[\mathrm{J \cdot x^{-1}}]$
n	Molar format:	$F_{\boldsymbol{n}\mathrm{mH^+}} \equiv \Delta\tilde{\mu}_{\mathrm{H+}}$	$=$	$F_{N\mathrm{mH^+}} \cdot N_\mathrm{A}$	$=$ $F_{\boldsymbol{e}\mathrm{mH^+}} \cdot (ze \cdot N_\mathrm{A})$	$[\mathrm{J \cdot mol^{-1}}]$
e	Electrical format:	$F_{\boldsymbol{e}\mathrm{mH^+}} \equiv \Delta p$	$=$	$F_{N\mathrm{mH^+}} \cdot (ze)^{-1}$	$=$ $F_{\boldsymbol{n}\mathrm{mH^+}} \cdot (ze \cdot N_\mathrm{A})^{-1}$	$[\mathrm{J \cdot C^{-1}}] \equiv [\mathrm{V}]$

The Faraday constant, $F = e \cdot N_\mathrm{A}$ $[\mathrm{C \cdot mol^{-1}}]$, is the product of elementary charge per particle, e $[\mathrm{C \cdot x^{-1}}]$, and the Avogadro (Loschmidt) constant, N_A $[\mathrm{x \cdot mol^{-1}}]$ (**Table 5**). Taken together, $ze \cdot N_\mathrm{A}$ is the conversion factor between electrical and chemical units. $F_{\boldsymbol{e}\mathrm{H^+}} \equiv \Delta p$ $[\mathrm{J \cdot C^{-1}}]$ is expressed per *motive charge* [C], whereas $F_{\boldsymbol{n}\mathrm{mH^+}} = \Delta p \cdot zF$ $[\mathrm{J \cdot mol^{-1}}]$ is expressed per *motive amount of protons* [mol] (**Table 4; Fig. 8**). The proton is the current-carrying entity (Kell 1979).

el: Electric part of the protonmotive force, three MU-formats

- ***N*** $F_{N\mathrm{el}}$, partial Gibbs energy change per *motive electron*, N_{e^-} $[\mathrm{J \cdot x^{-1}}]$.
- ***n*** $F_{\boldsymbol{n}\mathrm{el}} = \Delta\Psi \cdot zF$; electric force expressed in chemical units joule per mole $[\mathrm{J \cdot mol^{-1}}]$, defined as partial Gibbs energy change per *motive amount of electrons*, n_{e^-} [mol], not specific for proton charge.
- ***e*** $F_{\boldsymbol{e}\mathrm{el}} \equiv \Delta\Psi$; electric part of the protonmotive force expressed in electrical units joule per coulomb, *i.e.*, volt $[\mathrm{J \cdot C^{-1}} \equiv \mathrm{V}]$, defined as partial Gibbs energy change per *motive charge* [C], not specific for proton charge.

d: Chemical part (diffusion, d) of the protonmotive force, three MU-formats

- ***N*** $F_{N\mathrm{dH^+}}$, partial Gibbs energy change per *motive proton*, $N_{\mathrm{H^+}}$ $[\mathrm{J \cdot x^{-1}}]$.
- ***n*** $F_{\boldsymbol{n}\mathrm{dH^+}} \equiv \Delta\mu_{\mathrm{H^+}}$; chemical part (diffusion, translocation) of the protonmotive force expressed in units joule per mole $[\mathrm{J \cdot mol^{-1}}]$, defined as partial Gibbs energy change per *motive amount of protons*, n_H [mol].
- ***e*** $F_{\boldsymbol{e}\mathrm{dH^+}} = \Delta\mu_{\mathrm{H^+}} \cdot (zF)^{-1}$; chemical force expressed in units joule per coulomb $[\mathrm{J \cdot C^{-1}}]$, defined as partial Gibbs energy change per *motive amount of protons expressed in units of electric charge* [C], specific for the proton 'H' as the elemental entity.

Consider B^z as a cation that is permeable across the mtIM and is at equilibrium between the positive and negative compartments. The ionmotive force, $F_{\mathrm{mB}z}$, is zero at equilibrium, when the electric and chemical partial forces compensate each other (compare Eq. 2 in **Table 4**):

General:	$F_{\mathrm{mB}z} = F_\mathrm{el} + F_{\mathrm{dB}z}$	
At equilibrium: $F_{\mathrm{B}z} = 0$	$0 = F_\mathrm{el} + F_{\mathrm{dB}z}$	$F_\mathrm{el} = -F_{\mathrm{dB}z}$

For distribution of cation B^z between the negative and positive compartment (**Fig. 2**), an equilibrium concentration ratio (strictly activity ratio; **Table 6**) is obtained, $c_{\mathrm{B}z\mathrm{neg}}/c_{\mathrm{B}z\mathrm{pos}}$, the natural logarithm of which is $\Delta\ln c_{\mathrm{B}z} = \ln(c_{\mathrm{B}z\mathrm{neg}}/c_{\mathrm{B}z\mathrm{pos}})$. Multiplication of $\Delta\ln c_{\mathrm{B}z}$ by RT $[\mathrm{J \cdot mol^{-1}}]$ or kT $[\mathrm{J \cdot x^{-1}}]$ yields the partial chemical force, $F_{\mathrm{dB}z}$, as exergy per mole (format ***n***, based on the gas constant) or exergy per particle (format ***N***, based on the Boltzmann constant; **Table 5**). The MU-formats are interconverted as follows, considering equilibrium as described above:

N:	$F_{N\mathrm{el}}$	$=$ $\Delta\psi \cdot ze$	$= -F_{N\mathrm{dB}z}$	$= -RT \cdot N_\mathrm{A}^{-1}$	$\cdot\Delta\ln c_{\mathrm{B}z}$	$=$	$-kT$	$\cdot\Delta\ln c_{\mathrm{B}z}$
n:	$F_{\boldsymbol{n}\mathrm{el}}$	$=$ $\Delta\psi \cdot ze \cdot N_\mathrm{A}$	$= -F_{\boldsymbol{n}\mathrm{dB}z}$	$= -RT$	$\cdot\Delta\ln c_{\mathrm{B}z}$	$=$	$-kT \cdot N_\mathrm{A}$	$\cdot\Delta\ln c_{\mathrm{B}z}$
e:	$F_{\boldsymbol{e}\mathrm{el}}$	$\equiv$ $\Delta\psi$	$= -F_{\boldsymbol{e}\mathrm{dB}z}$	$= -RT \cdot (ze \cdot N_\mathrm{A})^{-1}$	$\cdot\Delta\ln c_{\mathrm{B}z}$	$=$	$-kT \cdot (ze)^{-1}$	$\cdot\Delta\ln c_{\mathrm{B}z}$

Due to the low permeability of the mtIM for protons and the action of the respiratory proton pumps, there is no equilibration of protons between the positive and negative compartments. Therefore, the protonmotive force, F_{mH^+}, is not zero, and F_{el} cannot be calculated from the proton distribution as described for the equilibrating cation B^z above. At zero ΔpH, $F_{mH^+} = F_{el}$ ($\Delta p = \Delta\psi$; Eq. 2). With·Δln c_{H^+} = -ln(10)·ΔpH = -2.3·ΔpH, the MU-formats for the chemical part of the protonmotive force are interconverted as described above, with z=1:

N:	$F_{N\mathrm{d}H^+}$	$= \Delta\mu_{H^+}\cdot N_A^{-1}$	$= RT\cdot N_A^{-1}$	$\cdot\Delta\ln c_{H^+}$	$= kT$	$\cdot\Delta\ln c_{H^+}$
n:	$F_{\boldsymbol{n}\mathrm{d}H^+}$	$\equiv \Delta\mu_{H^+}$	$= RT$	$\cdot\Delta\ln c_{H^+}$	$= kT\cdot N_A$	$\cdot\Delta\ln c_{H^+}$
e:	$F_{\boldsymbol{e}\mathrm{d}H^+}$	$= \Delta\mu_{H^+}\cdot(ze\cdot N_A)^{-1}$	$= RT\cdot(ze\cdot N_A)^{-1}$	$\cdot\Delta\ln c_{H^+}$	$= kT\cdot(ze)^{-1}$	$\cdot\Delta\ln c_{H^+}$

A partial electric force of 0.2 V in the electrical format, $F_{\boldsymbol{e}\mathrm{el,pos}}$ (**Table 6**, Note 5**e**), is 19 kJ·mol^{-1} H^+_{pos} in the molar format, $F_{\boldsymbol{n}\mathrm{el,pos}}$ (Note 5***n***). For 1 unit of ΔpH, the partial chemical force changes by -5.9 kJ·mol^{-1} in the molar format, $F_{\boldsymbol{n}\mathrm{dH^+pos}}$ (**Table 6**, Note 6***n***), and by -0.06 V in the electrical format, $F_{\boldsymbol{e}\mathrm{dH^+pos}}$ (Note 6***e***). Considering a driving force of -470 kJ·mol^{-1} O_2 for oxidation, the thermodynamic limit of the H^+_{pos}/O_2 ratio is reached at a value of 470/19 = 24, compared to a mechanistic stoichiometry of 20 (**Fig. 1**).

Table 4. Protonmotive force and flux matrix. Rows: Compartmental proton flux (rate) and protonmotive force (state). Molecular, molar and electrical formats (***N***, ***n*** and ***e***) with motive units, MU, of particle number, N [x], amount of substance, n [mol] and electric charge [C], respectively. Columns: The protonmotive force**,** F_{mH^+}**,** is the sum of two *partial isomorphic forces*, F_{el} + F_{dH^+}. In contrast to force, the conjugated flux cannot be partitioned but is expressed in different MU-formats.

State	Name	motive m	= electric el	+ chemical d	Unit	Notes
Rate	**Isomorphic flux**	J_{mH^+}			MU·s^{-1}·m^{-3}	1
	N molecular	$J_{\boldsymbol{N}mH^+}$			x·s^{-1}·m^{-3}	1***N***
	n molar	$J_{\boldsymbol{n}mH^+}$			mol·s^{-1}·m^{-3}	1***n***
	e electrical	$J_{\boldsymbol{e}mH^+}$			C·s^{-1}·m^{-3}	1***e***
State	**Isomorphic force**	F_{mH^+}	= F_{el}	+ F_{dH^+}	J·MU^{-1}	2
	N molecular	$F_{\boldsymbol{N}mH^+}$	= $F_{\boldsymbol{N}el}$	+ $F_{\boldsymbol{N}dH^+}$	J·x^{-1}	2***N***
	n molar	$F_{\boldsymbol{n}mH^+}$	= $F_{\boldsymbol{n}el}$	+ $F_{\boldsymbol{n}dH^+}$	J·mol^{-1}	2***n***
	e electrical	$F_{\boldsymbol{e}mH^+}$	= $F_{\boldsymbol{e}el}$	+ $F_{\boldsymbol{e}dH^+}$	J·C^{-1}	2***e***
	n Chemiosmotic potential	$\Delta\tilde{\mu}_{H^+}$	= $\Delta\Psi\cdot zF$	+ $\Delta\mu_{H^+}$	J·mol^{-1}	3***n***
	e Protonmotive force	Δp	= $\Delta\Psi$	+ $\Delta\mu_{H^+}/(zF)$	J·C^{-1}	3***e***

1: The sign of the flux, J_{mH^+}, depends on the definition of the compartmental direction of the translocation. Flux in the outward direction into the positively (pos) charged compartment, J_{mH^+pos}, is positive when H^+_{pos} is added to the pos-compartment (ν_{H^+pos} = 1), and H^+_{neg} is removed stoichiometrically (ν_{H^+neg} = -1). Conversely, J_{mH^+neg} is positive when H^+_{neg} is added to the negatively charged compartment (ν_{H^+neg} = 1) and H^+_{pos} is removed (ν_{H^+pos} = -1; **Fig. 2**).

2: F_{mH^+} is the protonmotive force expressed in any MU-format. F_{el} is the partial protonmotive force (el) acting generally on charged motive molecules (*i.e.*, ions that are permeable across the mtIM). In contrast, F_{dH^+} is the partial protonmotive force specific for proton diffusion (d) irrespective of charge. The sign of the force is negative for exergonic transformations in which exergy is lost or dissipated, F_{mH^+neg}, and positive for endergonic transformations which conserve exergy in a coupled exergonic process, $F_{mH^+pos} = -F_{mH^+neg}$ (**Box 3**). By definition, the product of flux and force is volume-specific power [J·s^{-1}·m^{-3} = W·m^{-3}]: $P_{V,mH^+} = J_{\boldsymbol{e}mH^+pos}\cdot F_{\boldsymbol{e}mH^+pos} = J_{\boldsymbol{n}mH^+pos}\cdot F_{\boldsymbol{n}mH^+pos}$.

3: 3***n*** and 3***e*** are the classical representations of 2***n*** ($F_{\boldsymbol{n}dH^+} \equiv \Delta\mu_{H^+}$) and 2***e*** ($F_{\boldsymbol{e}el} \equiv \Delta\Psi$). For further details see **Box 2**.

Table 5: Fundamental physical MU-formats, constants, and relationships

Format	Name	Abbreviation	Value (Gibney et al 2017)*	Unit
N	Molecular, particle			MU = x
n	Molar, chemical			MU = mol
e	Electrical			MU = C
N	Boltzmann constant*	k	$k = 1.380649 \cdot 10^{-23}$	$J \cdot x^{-1} \cdot K^{-1}$
n	Gas constant	$R = k \cdot N_A$	$k \cdot N_A = 8.31451$	$J \cdot mol^{-1} \cdot K^{-1}$
e	$R \cdot F^{-1} = k \cdot e^{-1}$ (*no name*)	$R \cdot F^{-1} = k \cdot e^{-1}$	$k \cdot e^{-1} = 8.617333 \cdot 10^{-5}$	$J \cdot C^{-1} \cdot K^{-1}$
N*/*n	Avogadro constant*	$N_A = N/n$	$N_A = 6.02214076 \cdot 10^{23}$	$x \cdot mol^{-1}$
e*/*N	Elementary charge*	e	$e = 1.602176634 \cdot 10^{-19}$	$C \cdot x^{-1}$
e*/*n	Faraday constant	$F = e \cdot N_A$	$e \cdot N_A = 96{,}485.33$	$C \cdot mol^{-1}$

Table 6. Power, exergy, force, flux, and advancement.

Expression	Symbol	Definition	Unit	Notes
Power, volume-specific	$P_{V,tr}$	$P_{V,tr} = J_{tr} \cdot F_{tr} = d_{tr}G \cdot dt^{-1} \cdot V^{-1}$	$J \cdot s^{-1} \cdot m^{-3}$	1
Force, isomorphic	F_{tr}	$F_{tr} = \partial G \cdot \partial_{tr}\xi^{-1}$	$J \cdot MU^{-1}$	2
Flux, isomorphic	J_{tr}	$J_{tr} = d_{tr}\xi \cdot dt^{-1} \cdot V^{-1}$	$MU \cdot s^{-1} \cdot m^{-3}$	3
Advancement, ***n***	$d_{tr}\xi_{\boldsymbol{n}H^+}$	$d_{tr}\xi_{\boldsymbol{n}H^+} = d_{tr}n_{H^+} \cdot \nu_{H^+}^{-1}$	MU=mol	4***n***
Advancement, ***e***	$d_{tr}\xi_{\boldsymbol{e}H^+}$	$d_{tr}\xi_{\boldsymbol{e}H^+} = d_{tr}e_{H^+} \cdot \nu_{H^+}^{-1}$	MU=C	4***e***
Electric partial force, ***n***	$F_{\boldsymbol{n}el}$	$F_{\boldsymbol{n}el} = \Delta\Psi \cdot zF = -RT \cdot \Delta \ln c_{Bz}$	$J \cdot mol^{-1}$	5***n***
at $z = 1$		$= 96.5 \cdot \Delta\Psi$	$kJ \cdot mol^{-1}$	
Electric partial force, ***e***	$F_{\boldsymbol{e}el}$	$F_{\boldsymbol{e}el} \equiv \Delta\Psi = -RT/(zF) \cdot \Delta \ln c_{Bz}$	$V = J \cdot C^{-1}$	5***e***
Chemical partial force, ***n***	$F_{\boldsymbol{n}dH^+}$	$F_{\boldsymbol{n}dH^+} \equiv \Delta\mu_{H^+} = -RT \cdot \ln(10) \cdot \Delta pH$	$J \cdot mol^{-1}$	6***n***
at 37 °C		$= -5.9 \cdot \Delta pH$	$kJ \cdot mol^{-1}$	
Chemical partial force, ***e***	$F_{\boldsymbol{e}dH^+}$	$F_{\boldsymbol{e}dH^+} = \Delta\mu_{H^+}/(zF) = -RT/(zF) \cdot \ln(10) \cdot \Delta pH$	$J \cdot C^{-1}$	6***e***
at 37 °C		$= -0.061 \cdot \Delta pH$	$J \cdot C^{-1}$	

1 to 4: The *SI* unit of power is watt [W ≡ $J \cdot s^{-1}$]. A motive entity, expressed in a motive unit [MU] is a characteristic for any type of transformation, tr.

2: Isomorphic forces, F_{tr}, are related to the generalized forces, X_{tr}, of irreversible thermodynamics as $F_{tr} = -X_{tr} \cdot T$, and the force of chemical reactions is the negative affinity, $F_r = -A$ (Prigogine 1967). ∂G [J] is the partial Gibbs energy (exergy) change in the advancement of transformation tr.

3: For MU = C, flow is electric current, I_{el} [A ≡ $C \cdot s^{-1}$], vector flux is electric current density per area, $\boldsymbol{J}_{el}$, and compartmental flux is electric current density per volume, I_{el} [$A \cdot m^{-3}$], all expressed in electrical format.

4: For a chemical reaction, the advancement of reaction r is $d_r\xi_B = d_r n_B \cdot \nu_B^{-1}$ [mol]. The stoichiometric number is $\nu_B = -1$ or $\nu_B = 1$, depending on B being a product or substrate, respectively, in reaction

r involving one mole of B. The conjugated *intensive* molar quantity, $F_{Br} = \partial G/\partial_r\xi_B$ [J·mol^{-1}], is the chemical force of reaction or *reaction-motive* force per stoichiometric amount of B. In reaction kinetics, $d_r n_B$ is expressed as a volume-specific quantity, which is the partial contribution to the total concentration change of B, $d_r c_B = d_r n_B/V$ and $dc_B = dn_B/V$, respectively. In open systems with constant volume V, $dc_B = d_r c_B + d_e c_B$, where r indicates the *internal* reaction and e indicates the *external* flux of B into the unit volume of the system. At steady state the concentration does not change, $dc_B = 0$, when $d_r c_B$ is compensated for by the external flux of B, $d_r c_B = -d_e c_B$ (Gnaiger 1993b). Alternatively, $dc_B = 0$ when B is held constant by different coupled reactions in which B acts as a substrate or a product.

5: Scalar potential difference across the mtIM. In a scalar electric transformation (flux of charge, *i.e.*, volume-specific current, from the matrix space to the intermembrane and extramitochondrial space), the motive force is the difference of charge (**Box 2**). The endergonic direction of translocation is defined in **Fig. 2** as $H^+_{neg} \rightarrow H^+_{pos}$. F = 96.5 (kJ·mol^{-1})/V (**Table 5**). z is the charge number of ion B. a_B is the (relative) activity of ion B, which in dilute solutions (c < 0.1 mol·dm^{-3}) is approximately equal to $c_B/c°$, where $c°$ is the standard concentration of 1 mol·dm^{-3}. Note that ion selective electrodes (pH or TPP$^+$ electrodes) respond to ln a_B. $\Delta \ln a_{H+} = -\ln(10)\cdot\Delta$pH (**Box 2**).

6: RT = 2.479 and 2.579 kJ·mol^{-1} at 298.15 and 310.15 K (25 and 37 °C), respectively (**Table 5**).

6***n***: ln(10)·RT = 5.708 and 5.938 kJ·mol^{-1} at 298.15 and 310.15 K, respectively. Replacing the gas constant, R, by the Boltzmann constant, k, converts the molar format, ***n*** [J·mol^{-1}] into the molecular format, ***N*** [J·x^{-1}] (**Box 2**).

6***e***: $RT/(zF)$ = 2.479 and 2.579 mV at 298.15 and 310.15 K, respectively, and ln(10)·$RT/(zF)$ = 59.16 and 61.54 mV, respectively, for z = 1.

3.2. Forces and fluxes in physics and thermodynamics

We place the concept of the protonmotive force into the general context of physical chemistry. Complementary to the attempt towards unification of fundamental forces defined in physics, the concepts of Nobel laureates Lars Onsager, Erwin Schrödinger, Ilya Prigogine and Peter Mitchell unite (even if expressed in apparently unrelated terms) the diversity of *generalized* or 'isomorphic' *flux-force* relationships, the product of which links to entropy production and the Second Law of thermodynamics (Schrödinger 1944; Prigogine 1967). A *motive force* is the derivative of potentially available or 'free' energy (exergy) per *motive elementary entity* (**Box 3**). Perhaps the first account of a *motive force* in energy transformation can be traced back to the Peripatetic school around 300 BC in the context of moving a lever, up to Newton's motive force proportional to the alteration of motion (Coopersmith 2010). As a generalization, isomorphic motive forces are considered as *entropic forces* in physics (Wang 2010).

Vectorial and scalar forces, and fluxes: In chemical reactions and osmotic or diffusion processes occurring in a closed heterogeneous system, such as a chamber containing isolated mitochondria, scalar transformations occur without measured spatial direction but between separate compartments (displacement between the negative and positive compartment; from the matrix to the intermembrane space) or between energetically-separated chemical substances (reactions proceeding from substrates to products). Hence, the corresponding fluxes are scalar but not vectorial, and are expressed per volume but not per membrane area (**Box 3**). The corresponding motive forces are also scalar potential *differences* across the membrane (**Table 6**), without taking into account the *gradients* across the 6 nm thick mtIM (Rich 2003).

Box 3: Metabolic fluxes and flows: vectorial and scalar

In mitochondrial electron transfer (**Fig. 1**), vectorial transmembrane proton flux is coupled through the proton pumps CI, CIII and CIV to the catabolic flux of scalar reactions, collectively measured as oxygen flux. In **Fig. 2**, the scalar catabolic reaction, k, of oxygen consumption, J_{kO_2} [mol·s^{-1}·m^{-3}], is expressed as oxygen flux per volume, V [m^3], of the instrumental chamber (the system).

Fluxes are *vectors*, if they have *spatial* direction in addition to magnitude. A vector flux (surface-density of flow) is expressed per unit cross-sectional area, A [m^2], perpendicular to the direction of flux. If *flows*, I, are defined as extensive quantities of the *system*, as vector or scalar flow, $\boldsymbol{I}$ or I [$mol \cdot s^{-1}$], respectively, then the corresponding vector and scalar *fluxes*, J, are obtained as $\boldsymbol{J} = \boldsymbol{I} \cdot A^{-1}$ [$mol \cdot s^{-1} \cdot m^{-2}$] and $J = I \cdot V^{-1}$ [$mol \cdot s^{-1} \cdot m^{-3}$], respectively, expressing flux as an area-specific vector or volume-specific scalar quantity.

Vectorial transmembrane proton fluxes, J_{mH^+pos} and J_{mH^+neg}, are analyzed in a heterogenous compartmental system as a quantity with *directional* but not *spatial* information. Translocation of protons across the mtIM has a defined direction, either from the negative compartment (matrix space; negative, neg-compartment) to the positive compartment (inter-membrane space; positive, pos-compartment) or *vice versa* (**Fig. 2**). The arrows defining the direction of the translocation between the two compartments may point upwards or downwards, right or left, without any implication that these are actual directions in space. The pos-compartment is neither above nor below the neg-compartment in a spatial sense, but can be visualized arbitrarily in a figure in the upper position (**Fig. 2**). In general, the *compartmental direction* of vectorial translocation from the neg-compartment to the pos-compartment is defined by assigning the initial and final state as *ergodynamic compartments*, $H^+_{neg} \rightarrow H^+_{pos}$ or $0 = -1\ H^+_{neg} + 1\ H^+_{pos}$, related to work (erg = work; **Box 4**) that must be performed to lift the proton from a lower to a higher electrochemical potential or from the lower to the higher ergodynamic compartment (Gnaiger 1993b).

In direct analogy to *vectorial* translocation, the direction of a *scalar* chemical reaction, $A \rightarrow B$ or $0 = -1\ A + 1\ B$, is defined by assigning substrates and products, A and B, as ergodynamic compartments. O_2 is defined as a substrate in respiratory O_2 consumption, which together with the fuel substrates comprises the substrate compartment of the catabolic reaction (**Fig. 2**). Volume-specific scalar O_2 flux is coupled (**Box 5**) to vectorial translocation. In order to establish a quantitative relation between the coupled fluxes, both J_{kO_2} and J_{mH^+pos} must be expressed in identical units, [$mol \cdot s^{-1} \cdot m^{-3}$] or [$C \cdot s^{-1} \cdot m^{-3}$], yielding the H^+_{pos}/O_2 ratio (**Fig. 1**). The *vectorial* proton flux in compartmental translocation has *compartmental direction*, distinguished from a *vector* flux with *spatial direction*. Likewise, the corresponding protonmotive force is defined as an electrochemical potential *difference* between two compartments, in contrast to a *gradient* across the membrane or a vector force with defined spatial direction.

Box 4: Endergonic and exergonic transformations, exergy and dissipation

A chemical reaction, and any transformation, is exergonic if the Gibbs energy change (exergy) of the reaction is negative at constant temperature and pressure. The sum of Gibbs energy changes of all internal transformations in a system can only be negative, *i.e.*, exergy is irreversibly dissipated. Endergonic reactions are characterized by positive Gibbs energies of reaction and cannot proceed spontaneously in the forward direction as defined. For instance, the endergonic reaction P» is coupled to exergonic catabolic reactions, such that the total Gibbs energy change is negative, *i.e.*, exergy must be dissipated for the reaction to proceed (**Fig. 2**).

In contrast, energy cannot be lost or produced in any internal process, which is the key message of the First Law of thermodynamics. Thus mitochondria are the sites of energy transformation but not energy production. Open and closed systems can gain energy and exergy only by external fluxes, *i.e.*, uptake from the environment. Exergy is the potential to perform work. In the framework of flux-force relationships (**Box 5**), the *partial* derivative of Gibbs energy per advancement of a transformation is an isomorphic force, F_{tr} (**Table 6**, Note 2). In other words, force is equal to exergy per motive entity (in integral form, this definition takes care of non-isothermal processes). This formal generalization represents an appreciation of the

conceptual beauty of Peter Mitchell's innovation of the protonmotive force against the background of the established paradigm of the electromotive force (emf) defined at the limit of zero current (Cohen *et al.* 2008).

Coupling: In energetics (ergodynamics), coupling is defined as an energy transformation fuelled by an exergonic (downhill) input process driving the advancement of an endergonic (uphill) output process. The (negative) output/input power ratio is the efficiency of a coupled energy transformation (**Box 5**). At the limit of maximum efficiency of a completely coupled system, the (negative) input power equals the (positive) output power, such that the total power approaches zero at the maximum efficiency of 1, and the process becomes fully reversible without any dissipation of exergy, *i.e.*, without entropy production.

Box 5: Coupling, power and efficiency, at constant temperature and pressure

Energetic coupling means that two processes of energy transformation are linked such that the input power, P_{in}, is the driving element of the output power, P_{out}, and the (negative) out/input power ratio is the efficiency. In general, power is work per unit time [$J \cdot s^{-1} \equiv W$]. When describing a system with volume V without information on the internal structure, the output is defined as the *external* work performed by the *total* system on its environment. Such a system may be open for any type of exchange, or closed and thus allowing only heat and work to be exchanged across the system boundaries. This is the classical black box approach of thermodynamics. In contrast, in a colourful compartmental analysis of *internal* energy transformations (**Fig. 2**), the system is structured and described by definition of ergodynamic compartments (with information on the heterogeneity of the system; **Box 3**) and analysis of separate parts, *i.e.*, a sequence of *partial* energy transformations, tr. At constant temperature and pressure, power per unit volume, $P_{V,tr} \equiv P_{tr}/V$ [$W \cdot m^{-3}$], is the product of a volume-specific flux, J_{tr}, and its conjugated force, F_{tr}, and is directly linked to entropy production, $d_iS/dt = \Sigma_{tr}P_{tr}/T$ [$W \cdot K^{-1}$], as generalized by irreversible thermodynamics (Prigogine 1967; Gnaiger 1993a,b). Output power of proton translocation and catabolic input power are (**Fig. 2**),

Output: $P_{mH^+pos}/V = J_{mH^+pos} \cdot F_{mH^+pos}$

Input: $P_{kO_2}/V = J_{kO_2} \cdot F_{kO_2}$

F_{kO_2} is the exergonic input force with a negative sign, and, F_{mH^+pos}, is the endergonic output force with a positive sign (**Box 4**). Ergodynamic efficiency is the ratio of output/input power, or the flux ratio times force ratio (Gnaiger 1993a,b),

$$\varepsilon = \frac{P_{mH^+pos}}{-P_{kO_2}} = \frac{J_{mH^+pos}}{J_{kO_2}} \cdot \frac{F_{mH^+pos}}{-F_{kO_2}}$$

The concept of incomplete coupling relates exclusively to the first term, *i.e.*, the flux ratio, or H^+_{pos}/O_2 ratio (**Fig. 1**). Likewise, respirometric definitions of the P»/O_2 ratio and biochemical coupling efficiency (Section 2.2) consider flux ratios. In a completely coupled process, the power efficiency, ε, depends entirely on the force ratio, ranging from zero efficiency at an output force of zero, to the limiting output force and maximum efficiency of 1.0, when the total power of the coupled process, $P_t = P_{kO_2} + P_{mH^+pos}$, equals zero, and any net flows are zero at ergodynamic equilibrium of a coupled process. Thermodynamic equilibrium is defined as the state when all potentials (all forces) are dissipated and equilibrate towards their minima of zero. In a fully or completely coupled process, output and input fluxes are directly proportional in a fixed ratio technically defined as a stoichiometric relationship (a gear ratio in a mechanical system). Such maximal stoichiometric output/input flux ratios are considered in OXPHOS analysis as the upper limits or mechanistic H^+_{pos}/O_2 and P»/O_2 ratios (**Fig. 1**).

Coupled versus bound processes: Since the chemiosmotic theory describes the mechanisms of coupling in OXPHOS, it may be interesting to ask if the electric and chemical parts of proton translocation are coupled processes. This is not the case according to the definition of coupling. If the coupling mechanism is disengaged, the output process becomes independent of the input process, and both proceed in their downhill (exergonic) direction (**Fig. 2**). It is not possible to physically uncouple the electric and chemical processes, which are only *theoretically* partitioned as electric and chemical components. The electric and chemical partial protonmotive *forces*, F_{el} and F_{dH^+}, can be measured separately. In contrast, the corresponding proton *flux*, J_{mH^+}, is non-separable, *i.e.*, cannot be uncoupled. Then these are not *coupled* processes, but are defined as *bound* processes. The electrical and chemical parts are tightly bound partial forces, since the flux cannot be partitioned (**Table 4**).

3.3. Absolute and relative measurements of the protonmotive force

4. Normalization: fluxes and flows

The challenges of measuring mitochondrial respiratory flux are matched by those of normalization. Application of common and generally defined units is required for direct transfer of reported results into a database. The second [s] is the *SI* unit for the base quantity *time*. It is also the standard time-unit used in solution chemical kinetics. A rate may be considered as the numerator and normalization as the complementary denominator, which are tightly linked in reporting the measurements in a format commensurate with the requirements of a database. MU-formats are simply converted to different *SI* units on the basis of physical constants (**Fig. 8**). In contrast, normalization (**Table 7**) is guided by physicochemical principles (**Fig. 9**), methodological considerations (**Fig. 10**), and conceptual strategies (**Fig. 11**).

4.1. Flux per chamber volume

When the reactor volume does not change during the reaction, which is typical for liquid phase reactions, the volume-specific *flux of a chemical reaction* r is the time derivative of the advancement of the reaction per unit volume, $J_{V,rB} = d_r\xi_B/dt \cdot V^{-1}$ [(mol·s^{-1})·L^{-1}]. The *rate of concentration change* is dc_B/dt [(mol·L^{-1})·s^{-1}], where concentration is $c_B = n_B/V$. It is important to make the fundamental distinction between (*1*) volume-specific flux [mol·s^{-1}·L^{-1}] and (*2*) rate of concentration change [mol·L^{-1}·s^{-1}]. These merge to a single expression only in closed systems. In open systems, external fluxes (such as O_2 supply) are distinguished from internal transformations (metabolic flux, O_2 consumption). In a closed system, external flows of all substances are zero and O_2 consumption (internal flow of katabolic reactions k), I_{kO_2} [pmol·s^{-1}], causes a decline of the amount of O_2 in the system, n_{O_2} [nmol]. Normalization of these quantities for the volume of the system, V [L ≡ dm^3], yields volume-specific O_2 flux, $J_{V,kO_2} = I_{kO_2}/V$ [nmol·s^{-1}·L^{-1}], and O_2 concentration, [O_2] or $c_{O_2} = n_{O_2}/V$ [µmol·L^{-1} = µM = nmol·mL^{-1}]. Instrumental background O_2 flux is due to external flux into a non-ideal closed respirometer, such that total volume-specific flux has to be corrected for instrumental background O_2 flux, *i.e.*, O_2 diffusion into or out of the instrumental chamber. J_{V,kO_2} is relevant mainly for methodological reasons and should be compared with the accuracy of instrumental resolution of background-corrected flux, *e.g.*, ±1 nmol·s^{-1}·L^{-1} (Gnaiger 2001). 'Metabolic' or catabolic indicates O_2 flux, J_{kO_2}, corrected for: (*1*) instrumental background O_2 flux; (*2*) chemical background O_2 flux due to autoxidation of chemical components added to the incubation medium; and (*3*) *Rox* for O_2-consuming side reactions unrelated to the catabolic pathway k.

4.2. System-specific and sample-specific normalization

The term *rate* is not sufficiently defined to be useful for a database (**Fig. 9**). The inconsistency of the meanings of rate becomes fully apparent when considering Galileo Galilei's famous principle, that 'bodies of different weight all fall at the same rate (have a constant acceleration)' (Coopersmith 2010).

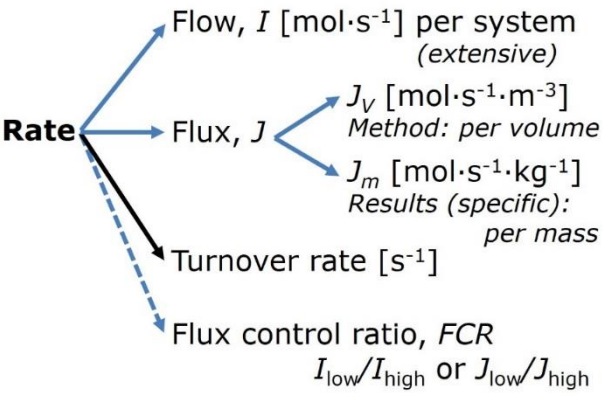

Fig. 9. Different meanings of *rate* may lead to confusion, if the normalization is not sufficiently specified. Results are frequently expressed as mass-specific *flux*, J_m, per mg protein, dry or wet weight (mass). Cell volume, V_{cell}, or mitochondrial volume, V_{mt}, may be used for normalization (volume-specific flux, J_{Vcell} or J_{Vmt}), which then must be clearly distinguished from flux, J_V, expressed for methodological reasons per volume of the measurement system, or flow per cell, I_X.

Extensive quantities: An extensive quantity increases proportionally with system size. The magnitude of an extensive quantity is completely additive for non-interacting subsystems, such as mass or flow expressed per defined system. The magnitude of these quantities depends on the extent or size of the system (Cohen *et al.* 2008).

Size-specific quantities: 'The adjective *specific* before the name of an extensive quantity is often used to mean *divided by mass*' (Cohen *et al.* 2008). Mass-specific flux is flow divided by mass of the system. A mass-specific quantity is independent of the extent of non-interacting homogenous subsystems. Tissue-specific quantities are of fundamental interest in comparative mitochondrial physiology, where *specific* refers to the *type* rather than *mass* of the tissue. The term *specific*, therefore, must be further clarified, such that tissue mass-specific, *e.g.*, muscle mass-specific quantities are defined.

Molar quantities: 'The adjective *molar* before the name of an extensive quantity generally means *divided by amount of substance*' (Cohen *et al.* 2008). The notion that all molar quantities then become *intensive* causes ambiguity in the meaning of *molar Gibbs energy*. It is important to emphasize the fundamental difference between normalization for amount of substance *in a system* or for amount of motive substance *in a transformation*. When the Gibbs energy of a system, G [J], is divided by the amount of substance B in the system, n_B [mol], a *size-specific* molar quantity is obtained, $G_B = G/n_B$ [J·mol^{-1}], which is not any force at all. In contrast, when the partial Gibbs energy change, ∂G [J], is divided by the motive amount of substance B in reaction r (advancement of reaction), $\partial_r\xi_B$ [mol], the resulting intensive molar quantity, $F_{rB} = \partial G/\partial_r\xi_B$ [J·mol^{-1}], is the chemical motive force of reaction r involving 1 mol B (**Table 6**, Note 4). These considerations apply not only to the molar format (**Fig. 8**).

Flow per system, *I*: In analogy to electrical terms, flow as an extensive quantity (I; per system) is distinguished from flux as a size-specific quantity (J; per system size) (**Fig. 9**). Electric current is flow, I_{el} [A ≡ C·s^{-1}] per system (extensive quantity). When dividing this extensive quantity by system size (membrane area), a size-specific quantity is obtained, which is electric flux (electric current density), $\boldsymbol{J}_{el}$ [A·m^{-2} = C·s^{-1}·m^{-2}].

Size-specific flux, *J*: Metabolic O_2 flow per tissue increases as tissue mass is increased. Tissue mass-specific O_2 flux should be independent of the size of the tissue sample studied in the instrument chamber, but volume-specific O_2 flux (per volume of the instrument chamber,

V) should increase in direct proportion to the amount of sample in the chamber. Accurate definition of the experimental system is decisive: whether the experimental chamber is the closed, open, isothermal or non-isothermal *system* with defined volume as part of the measurement apparatus, in contrast to the experimental *sample* in the chamber (**Table 7**). Volume-specific O_2 flux depends on mass-concentration of the sample in the chamber, but should be independent of the chamber volume. There are practical limitations to increasing the mass-concentration of the sample in the chamber, when one is concerned about crowding effects and instrumental time resolution.

Sample concentration, C_{mX}: Normalization for sample concentration is required for reporting respiratory data. Consider a tissue or cells as the sample, *X*, and the sample mass, m_X [mg] from which a mitochondrial preparation is obtained. m_X is frequently measured as wet or dry weight, W_w or W_d [mg], or as amount of tissue or cell protein, $m_{Protein}$. In the case of permeabilized tissues, cells, and homogenates, the sample concentration, $C_{mX} = m_X/V$ [mg·mL^{-1} = g·L^{-1}], is simply the mass of the subsample of tissue that is transferred into the instrument chamber. Part of the mitochondria from the tissue is lost during preparation of isolated mitochondria. The fraction of mitochondria obtained is expressed as mitochondrial recovery (**Fig. 10**). At a high mitochondrial recovery the sample of isolated mitochondria is more representative of the total mitochondrial population than in preparations characterized by low recovery. Determination of the mitochondrial recovery and yield is based on measurement of the concentration of a mitochondrial marker in the tissue homogenate, $C_{mte,thom}$, which simultaneously provides information on the specific mitochondrial density in the sample (**Fig. 10**).

Tissues can contain multiple cell populations which may have distinct mitochondrial subtypes. Mitochondria undergo dynamic fission and fusion cycles, and can exist in multiple stages and sizes which may be altered by a range of factors. The isolation of mitochondria (often achieved through differential centrifugation) can therefore yield a subsample of the mitochondrial types present in a tissue, dependent on isolation protocols utilized (*e.g.* centrifugation speed). This possible artefact should be taken into account when planning experiments using isolated mitochondria. The tendency for mitochondria of specific sizes to be enriched at different centrifugation speeds also has the potential to allow the isolation of specific mitochondrial subpopulations and therefore the analysis of mitochondria from multiple cell lineages within a single tissue.

Mass-specific flux, J_{mX,O_2}: Mass-specific flux is obtained by expressing respiration per mass of sample, m_X [mg]. *X* is the type of sample, *e.g.*, tissue homogenate, permeabilized fibres or cells. Volume-specific flux is divided by mass concentration of *X*, $J_{mX,O_2} = J_{V,O_2}/C_{mX}$; or flow per cell is divided by mass per cell, $J_{mcell,O_2} = I_{cell,O_2}/M_{cell}$. If mass-specific O_2 flux is constant and independent of sample size (expressed as mass), then there is no interaction between the subsystems. A 1.5 mg and a 3.0 mg muscle sample respires at identical mass-specific flux. Mass-specific O_2 flux, however, may change with the mass of a tissue sample, cells or isolated mitochondria in the measuring chamber, in which case the nature of the interaction becomes an issue. Optimization of cell density and arrangement is generally important and particularly in experiments carried out in wells, considering the confluency of the cell monolayer or clumps of cells (Salabei *et al.* 2014).

Number concentration, C_{NX}: C_{NX} is the experimental *number concentration* of sample *X*. In the case of cells or animals, *e.g.*, nematodes, $C_{NX} = N_X/V$ [x·L^{-1}], where N_X is the number of cells or organisms in the chamber (**Table 7**).

Table 7. Sample concentrations and normalization of flux with *SI* base units.

Expression	Symbol	Definition	*SI* Unit	Notes
Sample				
Identity of sample	X	Cells, animals, patients		
Number of sample entities X	N_X	Number of cells, *etc.*	x	
Mass of sample X	m_X		kg	1
Mass of entity X	M_X	$M_X = m_X \cdot N_X^{-1}$	$kg \cdot x^{-1}$	1
Mitochondria				
Mitochondria	mt	X = mt		
Amount of mt-elements	mte	Quantity of mt-marker	x_{mte}	
Concentrations				
Sample number concentration	C_{NX}	$C_{NX} = N_X \cdot V^{-1}$	$x \cdot m^{-3}$	2
Sample mass concentration	C_{mX}	$C_{mX} = m_X \cdot V^{-1}$	$kg \cdot m^{-3}$	
Mitochondrial concentration	C_{mte}	$C_{mte} = mte \cdot V^{-1}$	$x_{mte} \cdot m^{-3}$	3
Specific mitochondrial density	D_{mte}	$D_{mte} = mte \cdot m_X^{-1}$	$x_{mte} \cdot kg^{-1}$	4
Mitochondrial content, mte per entity X	mte_X	$mte_X = mte \cdot N_X^{-1}$	$x_{mte} \cdot x^{-1}$	5
O_2 flow and flux				6
Flow	I_{O_2}	Internal flow	$mol \cdot s^{-1}$	7
Volume-specific flux	J_{V,O_2}	$J_{V,O_2} = I_{O_2} \cdot V^{-1}$	$mol \cdot s^{-1} \cdot m^{-3}$	8
Flow per sample entity X	I_{X,O_2}	$I_{X,O_2} = J_{V,O_2} \cdot C_{NX}^{-1}$	$mol \cdot s^{-1} \cdot x^{-1}$	9
Mass-specific flux	J_{mX,O_2}	$J_{mX,O_2} = J_{V,O_2} \cdot C_{mX}^{-1}$	$mol \cdot s^{-1} \cdot kg^{-1}$	
Mitochondria-specific flux	J_{mte,O_2}	$J_{mte,O_2} = J_{V,O_2} \cdot C_{mte}^{-1}$	$mol \cdot s^{-1} \cdot x_{mte}^{-1}$	10

1 The *SI* prefix k is used for the SI base unit of mass (kg = 1,000 g). In praxis, various *SI* prefixes are used for convenience, to make numbers easily readable, *e.g.* 1 mg tissue, cell or mitochondrial mass instead of 0.000001 kg.

2 In case X = cells, the sample number concentration is $C_{Ncell} = N_{cell} \cdot V^{-1}$, and volume may be expressed in [$dm^3 \equiv L$] or [$cm^3 = mL$]. See **Table 8** for different sample types.

3 mt-concentration is an experimental variable, dependent on sample concentration: (*1*) $C_{mte} = mte \cdot V^{-1}$; (*2*) $C_{mte} = mte_X \cdot C_{NX}$; (*3*) $C_{mte} = C_{mX} \cdot D_{mte}$.

4 If the amount of mitochondria, mte, is expressed as mitochondrial mass, then D_{mte} is the mass fraction of mitochondria in the sample. If mte is expressed as mitochondrial volume, V_{mt}, and the mass of sample, m_X, is replaced by volume of sample, V_X, then D_{mte} is the volume fraction of mitochondria in the sample.

5 $mte_X = mte \cdot N_X^{-1} = C_{mte} \cdot C_{NX}^{-1}$.

6 O_2 can be replaced by other chemicals B to study different reactions, *e.g.* ATP, H_2O_2, or compartmental translocations, *e.g.* Ca^{2+}.

7 I_{O_2} and V are defined per instrument chamber as a system of constant volume (and constant temperature), which may be closed or open. I_{O_2} is abbreviated for I_{O_2r}, *i.e.*, the metabolic or internal O_2 flow of the chemical reaction r in which O_2 is consumed, hence the negative stoichiometric number, $\nu_{O_2} = -1$. $I_{O_2r} = d_r n_{O_2}/dt \cdot \nu_{O_2}^{-1}$. If r includes all chemical reactions in which O_2 participates, then $d_r n_{O_2} = dn_{O_2} - d_e n_{O_2}$, where dn_{O_2} is the change in the amount of O_2 in the instrument chamber and $d_e n_{O_2}$ is the amount of O_2 added externally to the system. At steady state, by definition $dn_{O_2} = 0$, hence $d_r n_{O_2} = -d_e n_{O_2}$.

8 J_{V,O_2} is an experimental variable, expressed per volume of the instrument chamber.

9 I_{X,O_2} is a physiological variable, depending on the size of entity X.

10 There are many ways to normalize for a mitochondrial marker, that are used in different experimental approaches: (*1*) $J_{mte,O_2} = J_{V,O_2} \cdot C_{mte}^{-1}$; (*2*) $J_{mte,O_2} = J_{V,O_2} \cdot C_{mX}^{-1} \cdot D_{mte}^{-1} = J_{mX,O_2} \cdot D_{mte}^{-1}$; (*3*) $J_{mte,O_2} = J_{V,O_2} \cdot C_{NX}^{-1} \cdot mte_X^{-1} = I_{X,O_2} \cdot mte_X^{-1}$; (*4*) $J_{mte,O_2} = I_{O_2} \cdot mte^{-1}$.

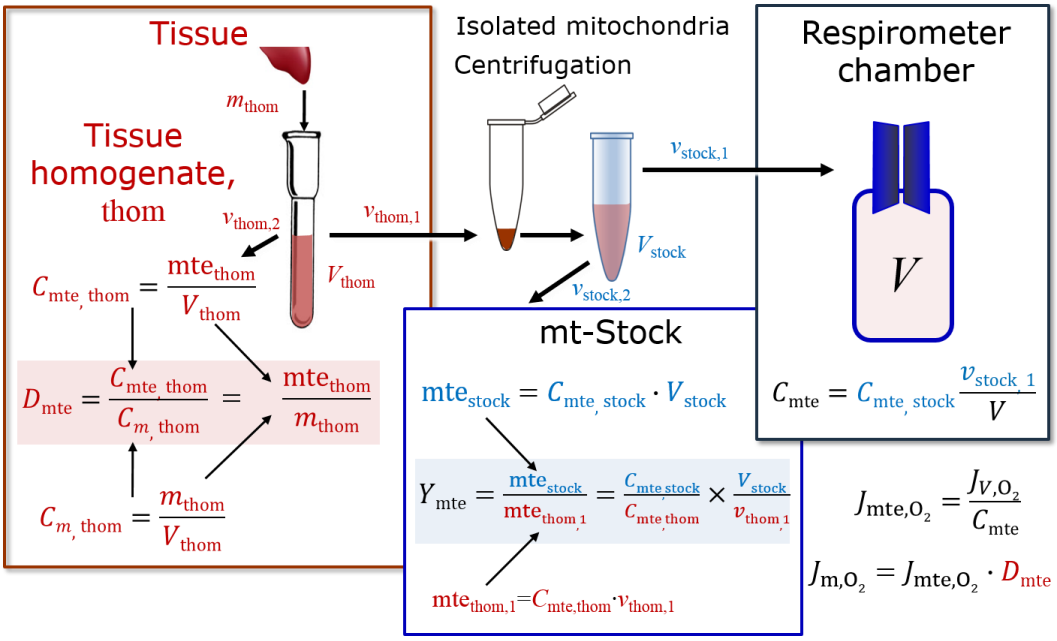

Symbol	Definition [Units]
C_{mte}	Mitochondrial concentration in chamber [$x_{mte} \cdot L^{-1}$]
C_m	Sample mass concentration in chamber [$g \cdot L^{-1}$]
D_{mte}	Specific mte-density per tissue mass [$x_{mte} \cdot g^{-1}$]
J_{m,O_2}	Mass-specific O_2 flux [$nmol \cdot s^{-1} \cdot g^{-1}$]
J_{mte,O_2}	Mitochondria-specific O_2 flux [$nmol \cdot s^{-1} \cdot x_{mte}^{-1}$]
mte	Amount of mitochondrial elements [x_{mte}]
m_{thom}	Mass of tissue in the homogenate [g]
Y_{mte}	Recovery of isolated mitochondria
$Y_{mte/m}$	Yield of isolated mitochondria; $Y_{mte/m} = Y_{mte} \cdot D_{mte}$ [$x_{mte} \cdot g^{-1}$]

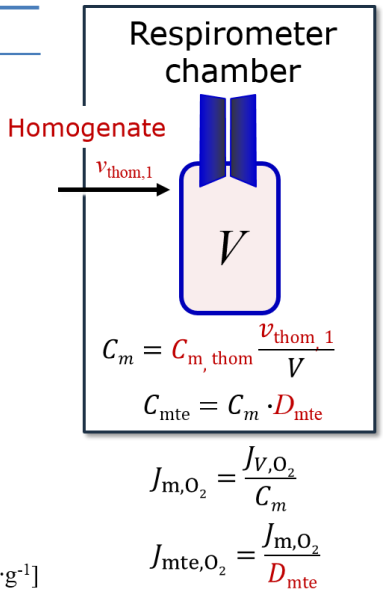

Fig. 10. Normalization of volume-specific flux of isolated mitochondria and tissue homogenate. A: Mitochondrial recovery, Y_{mte}, in preparation of isolated mitochondria. $v_{thom,1}$ and $v_{stock,1}$ are the volumes transferred from the total volume, V_{thom} and V_{stock}, respectively. $mte_{thom,1}$ is the amount of mitochondrial elements in volume $v_{thom,1}$ used for isolation. **B:** In respirometry with homogenate, $v_{thom,1}$ is transferred directly into the respirometer chamber. See **Table 7** for further explanation of symbols.

Flow per sample entity, I_{X,O_2}: A special case of normalization is encountered in respiratory studies with permeabilized (or intact) cells. If respiration is expressed per cell, the O_2 flow per measurement system is replaced by the O_2 flow per cell, I_{cell,O_2} (**Table 7**). O_2 flow can be calculated from volume-specific O_2 flux, J_{V,O_2} [$nmol \cdot s^{-1} \cdot L^{-1}$] (per V of the measurement chamber [L]), divided by the number concentration of cells, $C_{Nce} = N_{ce}/V$ [$cell \cdot L^{-1}$], where N_{ce} is the number of cells in the chamber. Cellular O_2 flow can be compared between cells of identical size. To take into account changes and differences in cell size, further normalization is required to obtain cell size-specific or mitochondrial marker-specific O_2 flux (Renner *et al.* 2003).

Table 8. Abbreviations of sample types, *X*.

Identity of sample	*X*
Mitochondrial preparation	mtprep
Isolated mitochondria	imt
Tissue homogenate	thom
Permeabilized tissue	pti
Permeabilized fibre	pfi
Permeabilized cell	pce
Cell	ce
Organism	org

The complexity changes when the sample is a whole organism studied as an experimental model. The well-established scaling law in respiratory physiology reveals a strong interaction of O_2 consumption and individual body mass of an organism, since *basal* metabolic rate (flow) does not increase linearly with body mass, whereas *maximum* mass-specific O_2 flux, $\dot{V}_{O2max}$ or $\dot{V}_{O2peak}$, is approximately constant across a large range of individual body mass (Weibel and Hoppeler 2005), with individuals, breeds, and certain species deviating substantially from this general relationship. $\dot{V}_{O2peak}$ of human endurance athletes is 60 to 80 mL $O_2 \cdot min^{-1} \cdot kg^{-1}$ body mass, converted to $J_{m,O2peak}$ of 45 to 60 $nmol \cdot s^{-1} \cdot g^{-1}$ (Gnaiger 2014; **Table 9**).

4.3. Normalization for mitochondrial content

Normalization is a problematic subject and it is essential to consider the question of the study. If the study aims to compare tissue performance, such as the effects of a certain treatment on a specific tissue, then normalization can be successful, using tissue mass or protein content, for example. If the aim, however, is to find differences of mitochondrial function independent of mitochondrial density (**Table 7**), then normalization to a mitochondrial marker is imperative (**Fig. 11**). However, one cannot assume that quantitative changes in various markers such as mitochondrial proteins necessarily occur in parallel with one another. It is important to first establish that the marker chosen is not selectively altered by the performed treatment. In conclusion, the normalization must reflect the question under investigation to reach a satisfying answer. On the other hand, the goal of comparing results across projects and institutions requires some standardization on normalization for entry into a databank.

Mitochondrial concentration, C_{mte}, and mitochondrial markers: It is important that mitochondrial concentration in the tissue and the measurement chamber be quantified, as a physiological output that is the result of mitochondrial biogenesis and degradation, and as a quantity for normalization in functional analyses. Mitochondrial organelles comprise a dynamic cellular reticulum in various states of fusion and fission. Hence the definition of an "amount" of mitochondria is often misconceived: mitochondria cannot be counted as a number of occurring elements. Therefore, quantification of the "amount" of mitochondria depends on measurement of chosen mitochondrial markers. ‘Mitochondria are the structural and functional elemental units of cell respiration’ (Gnaiger 2014). The quantity of a mitochondrial marker can be considered to reflect the amount of *elemental mitochondrial units* or *mitochondrial elements*, mte. However, since mitochondrial quality changes under certain stimuli, particularly in mitochondrial dysfunction and after exercise training (Pesta *et al.* 2011; Campos *et al.* 2017), some markers can vary while other markers are unchanged: (*1*) Mitochondrial volume and membrane area are structural markers, whereas mitochondrial protein mass is frequently used as a marker for isolated mitochondria. (*2*) Molecular and enzymatic mitochondrial markers (amounts or activities) can be selected as matrix markers, *e.g.*, citrate synthase activity, mtDNA;

mtIM-markers, *e.g.*, cytochrome *c* oxidase activity, aa_3 content, cardiolipin, or mtOM-markers, *e.g.*, TOM20. (*3*) Extending the measurement of mitochondrial marker enzyme activity to mitochondrial pathway capacity, ET- or OXPHOS-capacity can be considered as an integrative functional mitochondrial marker.

Depending on the type of mitochondrial marker, the mitochondrial elements, mte, are expressed in marker-specific units. It is recommended to distinguish *experimental mitochondrial concentration*, C_{mte} = mte/*V* and *physiological mitochondrial density*, D_{mte} = mte/m_X. Then mitochondrial density is the amount of mitochondrial elements per mass of tissue, which is a biological varible (**Fig. 11**). The experimental variable is mitochondrial density multiplied by sample mass concentration in the measuring chamber, $C_{mte} = D_{mte} \cdot C_{mX}$, or mitochondrial content multiplied by sample number concentration, $C_{mte} = mte_X \cdot C_{NX}$ (**Table 7**).

Mitochondria-specific flux, J_{mte,O_2}: Volume-specific metabolic O_2 flux depends on: (*1*) the sample concentration in the volume of the instrument chamber, C_{mX}, or C_{NX}; (*2*) the mitochondrial density in the sample, D_{mte} = mte/m_X or mte_X = mte/N_X; and (*3*) the specific mitochondrial activity or performance per elemental mitochondrial unit, $J_{mte,O_2} = J_{V,O_2}/C_{mte}$ (**Table 7**). Obviously, the numerical results for J_{mte,O_2} vary according to the type of mitochondrial marker chosen for measurement of mte and C_{mte} = mte/*V*.

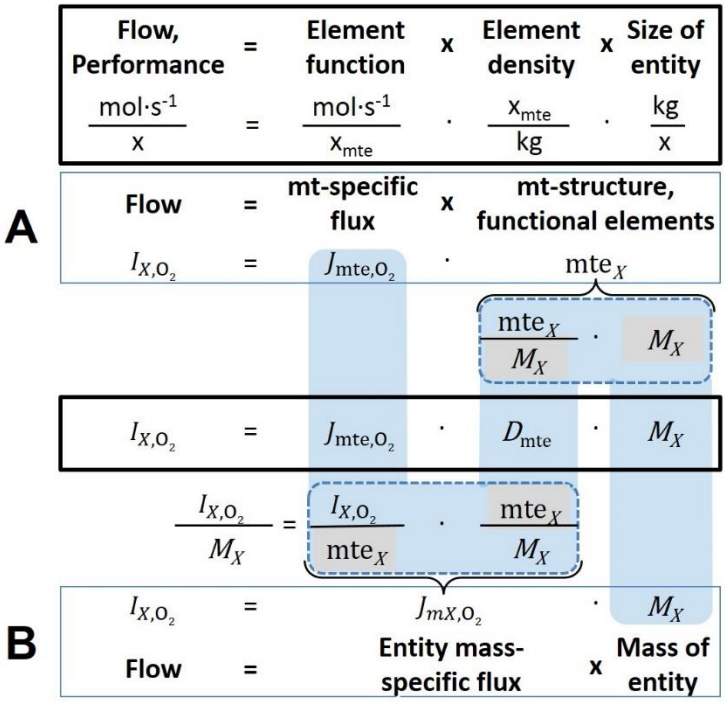

Fig. 11. Structure-function analysis of performance of an organism, organ or tissue, or a cell (sample entity, *X*). O_2 flow, I_{X,O_2}, is the product of performance per functional element (element function, mitochondria-specific flux), element density (mitochondrial density, D_{mte}), and size of entity *X* (mass, M_X). (**A**) Structured analysis: performance is the product of mitochondrial *function* (mt-specific flux) and *structure* (functional elements; D_{mte} times mass of *X*). (**B**) Unstructured analysis: performance is the product of *entity mass-specific flux*, $J_{mX,O_2} = I_{X,O_2}/M_X = I_{O_2}/m_X$ [mol·s^{-1}·kg^{-1}] and *size of entity*, expressed as mass of *X*; $M_X = m_X \cdot N_X^{-1}$ [kg·x^{-1}]. See **Table 7** for further explanation of quantities and units. Modified from Gnaiger (2014).

4.4. Evaluation of mitochondrial markers

Different methods are implicated in quantification of mitochondrial markers and have different strengths. Some problems are common for all mitochondrial markers, mte: (*1*)

Accuracy of measurement is crucial, since even a highly accurate and reproducible measurement of O_2 flux results in an inaccurate and noisy expression normalized for a biased and noisy measurement of a mitochondrial marker. This problem is acute in mitochondrial respiration because the denominators used (the mitochondrial markers) are often very small moieties whose accurate and precise determination is difficult. This problem can be avoided when O_2 fluxes measured in substrate-uncoupler-inhibitor titration protocols are normalized for flux in a defined respiratory reference state, which is used as an *internal* marker and yields flux control ratios, *FCR*s (**Fig. 9**). *FCR*s are independent of any *externally* measured markers and, therefore, are statistically very robust, considering the limitations of ratios in general (Jasienski and Bazzaz 1999). *FCR*s indicate qualitative changes of mitochondrial respiratory control, with highest quantitative resolution, separating the effect of mitochondrial density or concentration on J_{mX,O_2} and I_{X,O_2} from that of function per elemental mitochondrial marker, J_{mte,O_2} (Pesta *et al.* 2011; Gnaiger 2014). (*2*) If mitochondrial quality does not change and only the amount of mitochondria varies as a determinant of mass-specific flux, any marker is equally qualified in principle; then in practice selection of the optimum marker depends only on the accuracy and precision of measurement of the mitochondrial marker. (*3*) If mitochondrial flux control ratios change, then there may not be any best mitochondrial marker. In general, measurement of multiple mitochondrial markers enables a comparison and evaluation of normalization for a variety of mitochondrial markers. Particularly during postnatal development, the activity of marker enzymes, such as cytochrome *c* oxidase and citrate synthase, follows different time courses (Drahota *et al.* 2004). Evaluation of mitochondrial markers in healthy controls is insufficient for providing guidelines for application in the diagnosis of pathological states and specific treatments.

In line with the concept of the respiratory control ratio (Chance and Williams 1955a), the most readily used normalization is that of flux control ratios and flux control factors (Gnaiger 2014). Selection of the state of maximum flux in a protocol as the reference state has the advantages of: (*1*) internal normalization; (*2*) statistical linearization of the response in the range of 0 to 1; and (*3*) consideration of maximum flux for integrating a very large number of elemental steps in the OXPHOS- or ET-pathways. This reduces the risk of selecting a functional marker that is specifically altered by the treatment or pathodology, yet increases the chance that the highly integrative pathway is disproportionately affected, *e.g.* the OXPHOS- rather than ET-pathway in case of an enzymatic defect in the phosphorylation-pathway. In this case, additional information can be obtained by reporting flux control ratios based on a reference state which indicates stable tissue-mass specific flux. Stereological determination of mitochondrial content via two-dimensional transmission electron microscopy can have limitations due to the dynamics of mitochondrial size (Meinild Lundby *et al.* 2017). Accurate determination of three-dimensional volume by two-dimensional microscopy can be both time consuming and statistically challenging (Larsen *et al.* 2012).

The validity of using mitochondrial marker enzymes (citrate synthase activity, Complex I–IV amount or activity) for normalization of flux is limited in part by the same factors that apply to flux control ratios. Strong correlations between various mitochondrial markers and citrate synthase activity (Reichmann *et al.* 1985; Boushel *et al.* 2007; Mogensen *et al.* 2007) are expected in a specific tissue of healthy subjects and in disease states not specifically targeting citrate synthase. Citrate synthase activity is acutely modifiable by exercise (Tonkonogi *et al.* 1997; Leek *et al.* 2001). Evaluation of mitochondrial markers related to a selected age and sex cohort cannot be extrapolated to provide recommendations for normalization in respirometric diagnosis of disease, in different states of development and ageing, different cell types, tissues, and species. mtDNA normalised to nDNA via qPCR is correlated to functional mitochondrial markers including OXPHOS- and ET-capacity in some cases (Puntschart *et al.* 1995; Wang *et al.* 1999; Menshikova *et al.* 2006; Boushel *et al.* 2007), but lack of such correlations have been reported (Menshikova *et al.* 2005; Schultz and Wiesner

2000; Pesta *et al.* 2011). Several studies indicate a strong correlation between cardiolipin content and increase in mitochondrial function with exercise (Menshikova *et al.* 2005; Menshikova *et al.* 2007; Larsen *et al.* 2012; Faber *et al.* 2014), but its use as a general mitochondrial biomarker in disease remains questionable.

4.5. Conversion: units and normalization

Many different units have been used to report the rate of oxygen consumption, OCR (**Table 9**). *SI* base units provide the common reference for introducing the theoretical principles (**Fig. 9**), and are used with appropriately chosen *SI* prefixes to express numerical data in the most practical format, with an effort towards unification within specific areas of application (**Table 10**). For studies of cells, we recommend that respiration be expressed, as far as possible, as: (*1*) O_2 flux normalized for a mitochondrial marker, for separation of the effects of mitochondrial quality and content on cell respiration (this includes *FCR*s as a normalization for a functional mitochondrial marker); (*2*) O_2 flux in units of cell volume or mass, for comparison of respiration of cells with different cell size (Renner *et al.* 2003) and with studies on tissue preparations, and (*3*) O_2 flow in units of attomole (10^{-18} mol) of O_2 consumed in a second by each cell [amol·s^{-1}·cell^{-1}], numerically equivalent to [pmol·s^{-1}·10^{-6} cells]. This convention allows information to be easily used when designing experiments in which oxygen consumption must be considered. For example, to estimate the volume-specific O_2 flux in an instrument chamber that would be expected at a particular cell number concentration, one simply needs to multiply the flow per cell by the number of cells per volume of interest. This provides the amount of O_2 [mol] consumed per time [s^{-1}] per unit volume [L^{-1}]. At an O_2 flow of 100 amol·s^{-1}·cell^{-1} and a cell density of 10^9 cells·L^{-1} (10^6 cells·mL^{-1}), the volume-specific O_2 flux is 100 nmol·s^{-1}·L^{-1} (100 pmol·s^{-1}·mL^{-1}).

Table 9. Conversion of various units used in respirometry and ergometry. e is the number of electrons or reducing equivalents. z_B is the charge number of entity B.

1 Unit	x	Multiplication factor	*SI*-Unit	Note
ng.atom O·s^{-1}	(2 e$^-$)	0.5	nmol O_2·s^{-1}	
ng.atom O·min^{-1}	(2 e$^-$)	8.33	pmol O_2·s^{-1}	
natom O·min^{-1}	(2 e$^-$)	8.33	pmol O_2·s^{-1}	
nmol O_2·min^{-1}	(4 e$^-$)	16.67	pmol O_2·s^{-1}	
nmol O_2·h^{-1}	(4 e$^-$)	0.2778	pmol O_2·s^{-1}	
mL O_2·min^{-1} at STPD[a]		0.744	µmol O_2·s^{-1}	1
W = J/s at -470 kJ/mol O_2		-2.128	µmol O_2·s^{-1}	
mA = mC·s^{-1}	(z_{H^+} = 1)	10.36	nmol H^+·s^{-1}	2
mA = mC·s^{-1}	(z_{O_2} = 4)	2.59	nmol O_2·s^{-1}	2
nmol H^+·s^{-1}	(z_{H^+} = 1)	0.09649	mA	3
nmol O_2·s^{-1}	(z_{O_2} = 4)	0.38594	mA	3

1 At standard temperature and pressure dry (STPD: 0 °C = 273.15 K and 1 atm = 101.325 kPa = 760 mmHg), the molar volume of an ideal gas, V_m, and V_{m,O_2} is 22.414 and 22.392 L·mol^{-1} respectively. Rounded to three decimal places, both values yield the conversion factor of 0.744. For comparison at NTPD (20 °C), V_{m,O_2} is 24.038 L·mol^{-1}. Note that the *SI* standard pressure is 100 kPa.

2 The multiplication factor is $10^6/(z_B \cdot F)$.

3 The multiplication factor is $z_B \cdot F/10^6$.

Although volume is expressed as m^3 using the *SI* base unit, the litre [dm^3] is the basic unit of volume for concentration and is used for most solution chemical kinetics. If one multiplies I_{cell,O_2} by C_{Ncell}, then the result will not only be the amount of O_2 [mol] consumed per time [s^{-1}] in one litre [L^{-1}], but also the change in the concentration of oxygen per second (for any volume of an ideally closed system). This is ideal for kinetic modeling as it blends with chemical rate equations where concentrations are typically expressed in $mol \cdot L^{-1}$ (Wagner *et al.* 2011). In studies of multinuclear cells, such as differentiated skeletal muscle cells, it is easy to determine the number of nuclei but not the total number of cells. A generalized concept, therefore, is obtained by substituting cells by nuclei as the sample entity. This does not hold, however, for enucleated platelets.

J_{kO_2} is coupled in mitochondrial steady states to proton cycling, $J_{mH^+\infty} = J_{mH^+pos} = J_{mH^+neg}$ (**Fig. 2**). $J_{\boldsymbol{n}mH^+pos}$ and $J_{\boldsymbol{n}mH^+neg}$ [$nmol \cdot s^{-1} \cdot L^{-1}$] are converted into electrical units, $J_{\boldsymbol{e}mH^+pos}$ [$mC \cdot s^{-1} \cdot L^{-1} = mA \cdot L^{-1}$] = $J_{\boldsymbol{n}mH^+pos}$ [$nmol \cdot s^{-1} \cdot L^{-1}$]$\cdot zF$ [$C \cdot mol^{-1}$]$\cdot 10^{-6}$ (**Table 4**). At a J_{mH^+pos}/J_{kO_2} ratio or H^+_{pos}/O_2 of 20 (H^+_{pos}/O = 10), a volume-specific O_2 flux of 100 $nmol \cdot s^{-1} \cdot L^{-1}$ would correspond to a proton flux of 2,000 nmol $H^+_{pos} \cdot s^{-1} \cdot L^{-1}$ or volume-specific current of 193 $mA \cdot L^{-1}$.

$$J_{V,\boldsymbol{e}mH^+pos}\ [mA \cdot L^{-1}] = J_{V,\boldsymbol{n}mH^+pos} \cdot zF \cdot 10^{-6}\ [nmol \cdot s^{-1} \cdot L^{-1} \cdot mC \cdot nmol^{-1}] \quad (3.1)$$

$$J_{V,\boldsymbol{e}mH^+pos}\ [mA \cdot L^{-1}] = J_{V,O_2} \cdot (H^+_{pos}/O_2) \cdot zF \cdot 10^{-6}\ [mC \cdot s^{-1} \cdot L^{-1} = mA \cdot L^{-1}] \quad (3.2)$$

ET-capacity in various human cell types including HEK 293, primary HUVEC and fibroblasts ranges from 50 to 180 $amol \cdot s^{-1} \cdot cell^{-1}$, measured in intact cells in the noncoupled state (see Gnaiger 2014). At 100 $amol \cdot s^{-1} \cdot cell^{-1}$ corrected for *Rox* (corresponding to a catabolic power of -48 $pW \cdot cell^{-1}$), the current across the mt-membranes, $I_{\boldsymbol{e}H^+}$, approximates 193 $pA \cdot cell^{-1}$ or 0.2 nA per cell. See Rich (2003) for an extension of quantitative bioenergetics from the molecular to the human scale, with a transmembrane proton flux equivalent to 520 A in an adult at a catabolic power of -110 W. Modelling approaches illustrate the link between protonmotive force and currents (Willis *et al.* 2016).

Table 10. Conversion of units with preservation of numerical values.

Name	Frequently used unit	Equivalent unit	Note
Volume-specific flux, J_{V,O_2}	$pmol \cdot s^{-1} \cdot mL^{-1}$	$nmol \cdot s^{-1} \cdot L^{-1}$	1
	$mmol \cdot s^{-1} \cdot L^{-1}$	$mol \cdot s^{-1} \cdot m^{-3}$	
Cell-specific flow, I_{O_2}	$pmol \cdot s^{-1} \cdot 10^{-6}$ cells	$amol \cdot s^{-1} \cdot cell^{-1}$	2
	$pmol \cdot s^{-1} \cdot 10^{-9}$ cells	$zmol \cdot s^{-1} \cdot cell^{-1}$	3
Cell number concentration, C_{Nce}	10^6 cells$\cdot mL^{-1}$	10^9 cells$\cdot L^{-1}$	
Mitochondrial protein concentration, C_{mte}	0.1 $mg \cdot mL^{-1}$	0.1 $g \cdot L^{-1}$	
Mass-specific flux, J_{m,O_2}	$pmol \cdot s^{-1} \cdot mg^{-1}$	$nmol \cdot s^{-1} \cdot g^{-1}$	4
Catabolic power, P_k	$\mu W \cdot 10^{-6}$ cells	$pW \cdot cell^{-1}$	1
Volume	1,000 L	m^3 (1,000 kg)	
	L	dm^3 (kg)	
	mL	cm^3 (g)	
	µL	mm^3 (mg)	
	fL	μm^3 (pg)	5
Amount of substance concentration	M = $mol \cdot L^{-1}$	$mol \cdot dm^{-3}$	

1 pmol: picomole = 10^{-12} mol
2 amol: attomole = 10^{-18} mol
3 zmol: zeptomole = 10^{-21} mol
4 nmol: nanomole = 10^{-9} mol
5 fL: femtolitre = 10^{-15} L

We consider isolated mitochondria as powerhouses and proton pumps as molecular machines to relate experimental results to energy metabolism of the intact cell. The cellular P»/O_2 based on oxidation of glycogen is increased by the glycolytic (fermentative) substrate-level phosphorylation of 3 P»/Glyc, *i.e.*, 0.5 mol P» for each mol O_2 consumed in the complete oxidation of a mol glycosyl unit (Glyc). Adding 0.5 to the mitochondrial P»/O_2 ratio of 5.4 yields a bioenergetic cell physiological P»/O_2 ratio close to 6. Two NADH equivalents are formed during glycolysis and transported from the cytosol into the mitochondrial matrix, either by the malate-aspartate shuttle or by the glycerophosphate shuttle resulting in different theoretical yields of ATP generated by mitochondria, the energetic cost of which potentially must be taken into account. Considering also substrate-level phosphorylation in the TCA cycle, this high P»/O_2 ratio not only reflects proton translocation and OXPHOS studied in isolation, but integrates mitochondrial physiology with energy transformation in the living cell (Gnaiger 1993a).

5. Conclusions

MitoEAGLE can serve as a gateway to better diagnose mitochondrial respiratory defects linked to genetic variation, age-related health risks, sex-specific mitochondrial performance, lifestyle with its effects on degenerative diseases, and thermal and chemical environment. The present recommendations on coupling control states and rates, linked to the concept of the protonmotive force, are focused on studies with mitochondrial preparations. These will be extended in a series of reports on pathway control of mitochondrial respiration, respiratory states in intact cells, and harmonization of experimental procedures.

Box 6: Mitochondrial and cell respiration

Mitochondrial and cell respiration is the process of highly exergonic and exothermic energy transformation in which scalar redox reactions are coupled to vectorial ion translocation across a semipermeable membrane, which separates the small volume of a bacterial cell or mitochondrion from the larger volume of its surroundings. The electrochemical exergy can be partially conserved in the phosphorylation of ADP to ATP or in ion pumping, or dissipated in an electrochemical short-circuit. Respiration is thus clearly distinguished from fermentation as the counterpart of cellular core energy metabolism. Respiration is separated in mitochondrial preparations from the partial contribution of fermentative pathways of the intact cell. According to this definition, residual oxygen consumption, as measured after inhibition of mitochondrial electron transfer, does not belong to the class of catabolic reactions and is, therefore, subtracted from total oxygen consumption to obtain baseline-corrected respiration.

The optimal choice for expressing mitochondrial and cell respiration (**Box 6**) as O_2 flow per biological system, and normalization for specific tissue-markers (volume, mass, protein) and mitochondrial markers (volume, protein, content, mtDNA, activity of marker enzymes, respiratory reference state) is guided by the scientific question under study. Interpretation of the obtained data depends critically on appropriate normalization, and therefore reporting rates merely as nmol·s^{-1} is discouraged, since it restricts the analysis to intra-experimental comparison of relative (qualitative) differences. Expressing O_2 consumption per cell may not be possible when dealing with tissues. For studies with mitochondrial preparations, we recommend that normalizations be provided as far as possible: (*1*) on a per cell basis as O_2 flow (a biophysical normalization); (*2*) per g cell or tissue protein, or per cell or tissue mass as mass-specific O_2 flux (a cellular normalization); and (*3*) per mitochondrial marker as mt-specific flux (a mitochondrial normalization). With information on cell size and the use of multiple

normalizations, maximum potential information is available (Renner *et al.* 2003; Wagner *et al.* 2011; Gnaiger 2014).

Table 11. Alphabetical summary list of terms and symbols.

Term	Symbol	*SI* unit	Links and comments
Alternative quinol oxidase	AOX		Fig. 1
Amount of substance B	n_B	[mol]	Tab. 5
Apparent equilibrium constant	K_m'		
Charge number	z		Tab. 6; Tab. 9
Complexes I to IV	CI to CIV		Respiratory ET Complexes; Fig. 1
Concentration of substance B	$c_B = n_B \cdot V^{-1}$; [B]	[mol·m^{-3}]	Box 2, Tab. 6, Section 4.1
Diffusion, partial component	d		Tab. 4; chemical component
Electric, partial component	el		Tab. 4
Electrical format	***e***	[C]	Fig. 8
Electron	e$^-$	[x]	Tab. 9
Electron transfer system	ETS		
Flow, for substance B	I_B	[MU·s^{-1}]	System-related, extensive quantity; Fig. 9
Flux, for substance B	J_B		Size-specific quantitiy; Fig. 9, Tab. 6
Force, isomorphic, per B	F_{Btr}	[J·MU^{-1}]	Tab. 6, Box 4; force of transformation tr. tr must be defined, *e.g.*, as a chemical reaction, r, or diffusion, d.
Inorganic phosphate	P_i		
Proton in the negative compartment	H^+_{neg}		Fig. 2
Proton in the positive compartment	H^+_{pos}		Fig. 2
LEAK	LEAK		Tab. 1
Mass of sample *X*	m_X	[kg]	Tab. 7
Mass of entity *X*	M_X	[kg]	Tab. 7
MITOCARTA			https://www.broadinstitute.org/scientific-community/science/programs/metabolic-disease-program/publications/mitocarta/mitocarta-in-0
Meitochondria or mitochondrial	mt		Box 1
Mitochondrial DNA	mtDNA		Box 1
Mitochondrial inner membrane	mtIM		MIM is widely used, and M is replaced by mt as abbreviation for mitochondria; Box 1
Mitochondrial outer membrane	mtOM		MOM is widely used, and M is replaced by mt as abbreviation for mitochondria; Box 1
Mitochondrial concentration	$C_{mte} = mte \cdot V^{-1}$	[x_{mte}·m^{-3}]	Tab. 7
Mitochondrial content	$mte_X = mte \cdot N_X^{-1}$	[x_{mte}·x^{-1}]	Tab. 7
Mitochondrial recovery	Y_{mte}		Fig. 10
Mitochondrial yield	$Y_{mte/m}$		Fig. 10
Molecular format	***N***	[x]	Fig. 8
Molar format	***n***	[mol]	Fig. 8
Motive, total	m		Tab. 4; motive = electric + chemical
Motive unit	MU	*varies*	Fig. 8
Negative	neg		Fig. 2
Number concentration of *X*	C_{NX}	[x·m^{-3}]	Tab. 7
Number of entities *X*	N_X	[x]	Tab. 7, Fig. 11
Number of molecules B	N_B	[x]	Fig. 8. According to IUPAC, the unit of N is "1", but the Avogadro constant, $N_A = N/n$, has the IUPAC unit [mol^{-1}] rather than [1·mol^{-1}]. For consistency, we

			suggest the unit [x] for N and [x·mol^{-1}] for N_A (Tab. 5).
Oxidative phosphorylation	OXPHOS		Tab. 1
Oxygen concentration	$c_{O2} = n_{O2} \cdot V^{-1}$; [$O_2$]	[mol·m^{-3}]	Section 4.1
Phosphorylation of ADP to ATP	P»		
Positive	pos		Fig. 2
Power of energy transformation, tr	P_{tr}		Tab. 6
Protonmotive force	F_{mH+}	[J·MU^{-1}]	Tab. 4
Rate of electron transfer in ET state	E		ET-capacity; Tab. 1
Rate of LEAK respiration	L		Tab. 1
Rate of oxidative phosphorylation	P		OXPHOS capacity; Tab. 1
Rate of residual oxygen consumption	Rox		Tab. 1
Residual oxygen consumption	ROX		Tab. 1
Specific mitochondrial density	$D_{mte} = mte \cdot m_X^{-1}$	[xmte·kg^{-1}]	Tab. 7
Volume	V	[m^{-3}]	
Weight, dry weight	W_d	[kg]	Used as mass of sample X; Fig. 9
Weight, wet weight	W_w	[kg]	Used as mass of sample X; Fig. 9

When using isolated mitochondria, mitochondrial protein is a frequently applied mitochondrial marker, the use of which is basically restricted to isolated mitochondria. The mitochondrial recovery and yield, and experimental criteria for evaluation of purity versus integrity should be reported. Mitochondrial markers, such as citrate synthase activity as an enzymatic matrix marker, provide a link to the tissue of origin on the basis of calculating the mitochondrial recovery, *i.e.*, the fraction of mitochondrial marker obtained from a unit mass of tissue.

Molecular, molar or electrical formats can be chosen for reporting metabolic fluxes and the motive forces. The motive entities are expressed in *SI* units corresponding to these formats (pure number, mole, coulomb). The molar or chemical format, ***n***, is most commonly used for reporting metabolic fluxes and concentrations in solution chemical kinetics, whereas the protonmotive force is more frequently expressed in the electrical format, ***e***. The molecular or particle format, ***N***, is based on counting the number of occurring elements, which is not practicable for mitochondria in their dynamic states of fusion and fission, but is standard for most cell types. A number concentration of 10^9 cells·L^{-1} is hardly ever expressed in the molar format of 1.66 fmol cells·L^{-1}. When O_2 flow is given as 100 amol·s^{-1}·cell^{-1}, a mixed ***n***/***N*** format is used. $60.2 \cdot 10^6$ mol O_2·s^{-1}·mol^{-1} cells is equivalent to $60.2 \cdot 10^6$ molecules O_2·s^{-1}·cell^{-1} and represents a consistent ***n***/***n*** or ***N***/***N*** format, which is - perhaps surprisingly - not familiar and hardly ever used. The variety of formats is large and sufficiently confusing even on the basis of *SI* units. To avoid further complicating the field of mitochondrial physiology, therefore, strict adherence to *SI* units is mandatory. Furthermore, the chemical format with the motive unit *mole* has the highest chance of general acceptance in cell metabolism and mitochondrial physiology. Taken together, this evaluation provides a strong argument for a recommendation to report respiratory rates, including scalar and vectorial flows and fluxes, and states, including the protonmotive force, in a common chemical format for entry into any database. Terms and symbols are summarized in **Table 11**, the use of which is recommended for reporting results on the protonmotive force and respiratory control. This will facilitate transdisciplinary communication and support further developments towards a consistent theory of bioenergetics and mitochondrial physiology.

Acknowledgements

We thank M. Beno for management assistance. Supported by COST Action CA15203 MitoEAGLE and K-Regio project MitoFit (E.G.).

Competing financial interests: E.G. is founder and CEO of Oroboros Instruments, Innsbruck, Austria.

6. References

Altmann R (1894) Die Elementarorganismen und ihre Beziehungen zu den Zellen. Zweite vermehrte Auflage. Verlag Von Veit & Comp, Leipzig:160 pp.

Beard DA (2005) A biophysical model of the mitochondrial respiratory system and oxidative phosphorylation. PLoS Comput Biol 1(4):e36.

Benda C (1898) Weitere Mitteilungen über die Mitochondria. Verh Dtsch Physiol Ges:376-83.

Birkedal R, Laasmaa M, Vendelin M (2014) The location of energetic compartments affects energetic communication in cardiomyocytes. Front Physiol 5:376.

Breton S, Beaupré HD, Stewart DT, Hoeh WR, Blier PU (2007) The unusual system of doubly uniparental inheritance of mtDNA: isn't one enough? Trends Genet 23:465-74.

Brown GC (1992) Control of respiration and ATP synthesis in mammalian mitochondria and cells. Biochem J 284:1-13.

Calvo SE, Klauser CR, Mootha VK (2016) MitoCarta2.0: an updated inventory of mammalian mitochondrial proteins. Nucleic Acids Research 44:D1251-7.

Calvo SE, Julien O, Clauser KR, Shen H, Kamer KJ, Wells JA, Mootha VK (2017) Comparative analysis of mitochondrial N-termini from mouse, human, and yeast. Mol Cell Proteomics 16:512-23.

Campos JC, Queliconi BB, Bozi LHM, Bechara LRG, Dourado PMM, Andres AM, Jannig PR, Gomes KMS, Zambelli VO, Rocha-Resende C, Guatimosim S, Brum PC, Mochly-Rosen D, Gottlieb RA, Kowaltowski AJ, Ferreira JCB (2017) Exercise reestablishes autophagic flux and mitochondrial quality control in heart failure. Autophagy 13:1304-317.

Canton M, Luvisetto S, Schmehl I, Azzone GF (1995) The nature of mitochondrial respiration and discrimination between membrane and pump properties. Biochem J 310:477-81.

Chance B, Williams GR (1955a) Respiratory enzymes in oxidative phosphorylation. I. Kinetics of oxygen utilization. J Biol Chem 217:383-93.

Chance B, Williams GR (1955b) Respiratory enzymes in oxidative phosphorylation: III. The steady state. J Biol Chem 217:409-27.

Chance B, Williams GR (1955c) Respiratory enzymes in oxidative phosphorylation. IV. The respiratory chain. J Biol Chem 217:429-38.

Chance B, Williams GR (1956) The respiratory chain and oxidative phosphorylation. Adv Enzymol Relat Subj Biochem 17:65-134.

Cobb LJ, Lee C, Xiao J, Yen K, Wong RG, Nakamura HK, Mehta HH, Gao Q, Ashur C, Huffman DM, Wan J, Muzumdar R, Barzilai N, Cohen P (2016) Naturally occurring mitochondrial-derived peptides are age-dependent regulators of apoptosis, insulin sensitivity, and inflammatory markers. Aging (Albany NY) 8:796-809.

Cohen ER, Cvitas T, Frey JG, Holmström B, Kuchitsu K, Marquardt R, Mills I, Pavese F, Quack M, Stohner J, Strauss HL, Takami M, Thor HL (2008) Quantities, units and smbols in physical chemistry, IUPAC Green Book, 3rd Edition, 2nd Printing, IUPAC & RSC Publishing, Cambridge.

Cooper H, Hedges LV, Valentine JC, eds (2009) The handbook of research synthesis and meta-analysis. Russell Sage Foundation.

Coopersmith J (2010) Energy, the subtle concept. The discovery of Feynman's blocks from Leibnitz to Einstein. Oxford University Press:400 pp.

Cummins J (1998) Mitochondrial DNA in mammalian reproduction. Rev Reprod 3:172-82.

Dai Q, Shah AA, Garde RV, Yonish BA, Zhang L, Medvitz NA, Miller SE, Hansen EL, Dunn CN, Price TM (2013) A truncated progesterone receptor (PR-M) localizes to the mitochondrion and controls cellular respiration. Mol Endocrinol 27:741-53.

Divakaruni AS, Brand MD (2011) The regulation and physiology of mitochondrial proton leak. Physiology (Bethesda) 26:192-205.

Doerrier C, Garcia-Souza LF, Krumschnabel G, Wohlfarter Y, Mészáros AT, Gnaiger E (2018) High-Resolution FluoRespirometry and OXPHOS protocols for human cells, permeabilized fibres from small biopsies of muscle and isolated mitochondria. Methods Mol. Biol. (in press)

Doskey CM, van 't Erve TJ, Wagner BA, Buettner GR (2015) Moles of a substance per cell is a highly informative dosing metric in cell culture. PLOS ONE 10:e0132572.

Drahota Z, Milerová M, Stieglerová A, Houstek J, Ostádal B (2004) Developmental changes of cytochrome *c* oxidase and citrate synthase in rat heart homogenate. Physiol Res 53:119-22.

Duarte FV, Palmeira CM, Rolo AP (2014) The role of microRNAs in mitochondria: small players acting wide. Genes (Basel) 5:865-86.

Ernster L, Schatz G (1981) Mitochondria: a historical review. J Cell Biol 91:227s-55s.

1799 Estabrook RW (1967) Mitochondrial respiratory control and the polarographic measurement of ADP:O ratios.
1800 Methods Enzymol 10:41-7.
1801 Faber C, Zhu ZJ, Castellino S, Wagner DS, Brown RH, Peterson RA, Gates L, Barton J, Bickett M, Hagerty L,
1802 Kimbrough C, Sola M, Bailey D, Jordan H, Elangbam CS (2014) Cardiolipin profiles as a potential
1803 biomarker of mitochondrial health in diet-induced obese mice subjected to exercise, diet-restriction and
1804 ephedrine treatment. J Appl Toxicol 34:1122-9.
1805 Fell D (1997) Understanding the control of metabolism. Portland Press.
1806 Garlid KD, Beavis AD, Ratkje SK (1989) On the nature of ion leaks in energy-transducing membranes. Biochim
1807 Biophys Acta 976:109-20.
1808 Garlid KD, Semrad C, Zinchenko V. Does redox slip contribute significantly to mitochondrial respiration? In:
1809 Schuster S, Rigoulet M, Ouhabi R, Mazat J-P, eds (1993) Modern trends in biothermokinetics. Plenum Press,
1810 New York, London:287-93.
1811 Gerö D, Szabo C (2016) Glucocorticoids suppress mitochondrial oxidant production via upregulation of
1812 uncoupling protein 2 in hyperglycemic endothelial cells. PLoS One 11:e0154813.
1813 Gibney E (2017) New definitions of scientific units are on the horizon. Nature 550:312–13.
1814 Gnaiger E. Efficiency and power strategies under hypoxia. Is low efficiency at high glycolytic ATP production a
1815 paradox? In: Surviving Hypoxia: Mechanisms of Control and Adaptation. Hochachka PW, Lutz PL, Sick T,
1816 Rosenthal M, Van den Thillart G, eds (1993a) CRC Press, Boca Raton, Ann Arbor, London, Tokyo:77-109.
1817 Gnaiger E (1993b) Nonequilibrium thermodynamics of energy transformations. Pure Appl Chem 65:1983-2002.
1818 Gnaiger E (2001) Bioenergetics at low oxygen: dependence of respiration and phosphorylation on oxygen and
1819 adenosine diphosphate supply. Respir Physiol 128:277-97.
1820 Gnaiger E (2009) Capacity of oxidative phosphorylation in human skeletal muscle. New perspectives of
1821 mitochondrial physiology. Int J Biochem Cell Biol 41:1837-45.
1822 Gnaiger E (2014) Mitochondrial pathways and respiratory control. An introduction to OXPHOS analysis. 4th ed.
1823 Mitochondr Physiol Network 19.12. Oroboros MiPNet Publications, Innsbruck:80 pp.
1824 Gnaiger E, Méndez G, Hand SC (2000) High phosphorylation efficiency and depression of uncoupled respiration
1825 in mitochondria under hypoxia. Proc Natl Acad Sci USA 97:11080-5.
1826 Greggio C, Jha P, Kulkarni SS, Lagarrigue S, Broskey NT, Boutant M, Wang X, Conde Alonso S, Ofori E,
1827 Auwerx J, Cantó C, Amati F (2017) Enhanced respiratory chain supercomplex formation in response to
1828 exercise in human skeletal muscle. Cell Metab 25:301-11.
1829 Hinkle PC (2005) P/O ratios of mitochondrial oxidative phosphorylation. Biochim Biophys Acta 1706:1-11.
1830 Hofstadter DR (1979) Gödel, Escher, Bach: An eternal golden braid. A metaphorical fugue on minds and
1831 machines in the spirit of Lewis Carroll. Harvester Press:499 pp.
1832 Illaste A, Laasmaa M, Peterson P, Vendelin M (2012) Analysis of molecular movement reveals latticelike
1833 obstructions to diffusion in heart muscle cells. Biophys J 102:739-48.
1834 Jasienski M, Bazzaz FA (1999) The fallacy of ratios and the testability of models in biology. Oikos 84:321-26.
1835 Jepihhina N, Beraud N, Sepp M, Birkedal R, Vendelin M (2011) Permeabilized rat cardiomyocyte response
1836 demonstrates intracellular origin of diffusion obstacles. Biophys J 101:2112-21.
1837 Kell DB (1979) On the functional proton current pathway of electron transport phosphorylation: An electrodic
1838 view. Biochim Biophys Acta 549:55-99.
1839 Klepinin A, Ounpuu L, Guzun R, Chekulayev V, Timohhina N, Tepp K, Shevchuk I, Schlattner U, Kaambre T
1840 (2016) Simple oxygraphic analysis for the presence of adenylate kinase 1 and 2 in normal and tumor cells. J
1841 Bioenerg Biomembr 48:531-48.
1842 Klingenberg M (2017) UCP1 - A sophisticated energy valve. Biochimie 134:19-27.
1843 Koit A, Shevchuk I, Ounpuu L, Klepinin A, Chekulayev V, Timohhina N, Tepp K, Puurand M,Truu L, Heck K,
1844 Valvere V, Guzun R, Kaambre T (2017) Mitochondrial respiration in human colorectal and breast cancer
1845 clinical material is regulated differently. Oxid Med Cell Longev 1372640.
1846 Komlódi T, Tretter L (2017) Methylene blue stimulates substrate-level phosphorylation catalysed by succinyl-
1847 CoA ligase in the citric acid cycle. Neuropharmacology 123:287-98.
1848 Lane N (2005) Power, sex, suicide: mitochondria and the meaning of life. Oxford University Press:354 pp.
1849 Larsen S, Nielsen J, Neigaard Nielsen C, Nielsen LB, Wibrand F, Stride N, Schroder HD, Boushel RC, Helge
1850 JW, Dela F, Hey-Mogensen M (2012) Biomarkers of mitochondrial content in skeletal muscle of healthy
1851 young human subjects. J Physiol 590:3349-60.
1852 Lee C, Zeng J, Drew BG, Sallam T, Martin-Montalvo A, Wan J, Kim SJ, Mehta H, Hevener AL, de Cabo R,
1853 Cohen P (2015) The mitochondrial-derived peptide MOTS-c promotes metabolic homeostasis and reduces
1854 obesity and insulin resistance. Cell Metab 21:443-54.
1855 Lee SR, Kim HK, Song IS, Youm J, Dizon LA, Jeong SH, Ko TH, Heo HJ, Ko KS, Rhee BD, Kim N, Han J
1856 (2013) Glucocorticoids and their receptors: insights into specific roles in mitochondria. Prog Biophys Mol
1857 Biol 112:44-54.
1858 Leek BT, Mudaliar SR, Henry R, Mathieu-Costello O, Richardson RS (2001) Effect of acute exercise on citrate
1859 synthase activity in untrained and trained human skeletal muscle. Am J Physiol Regul Integr Comp Physiol
1860 280:R441-7.

1861 Lemieux H, Blier PU, Gnaiger E (2017) Remodeling pathway control of mitochondrial respiratory capacity by
1862 temperature in mouse heart: electron flow through the Q-junction in permeabilized fibers. Sci Rep 7:2840.
1863 Lenaz G, Tioli G, Falasca AI, Genova ML (2017) Respiratory supercomplexes in mitochondria. In: Mechanisms
1864 of primary energy trasduction in biology. M Wikstrom (ed) Royal Society of Chemistry Publishing, London,
1865 UK:296-337.
1866 Margulis L (1970) Origin of eukaryotic cells. New Haven: Yale University Press.
1867 Meinild Lundby AK, Jacobs RA, Gehrig S, de Leur J, Hauser M, Bonne TC, Flück D, Dandanell S, Kirk N,
1868 Kaech A, Ziegler U, Larsen S, Lundby C (2017) Exercise training increases skeletal muscle mitochondrial
1869 volume density by enlargement of existing mitochondria and not de novo biogenesis. Acta Physiol (Oxf)
1870 [Epub ahead of print].
1871 Menshikova EV, Ritov VB, Fairfull L, Ferrell RE, Kelley DE, Goodpaster BH (2006) Effects of exercise on
1872 mitochondrial content and function in aging human skeletal muscle. J Gerontol A Biol Sci Med Sci 61:534-
1873 40.
1874 Menshikova EV, Ritov VB, Ferrell RE, Azuma K, Goodpaster BH, Kelley DE (2007) Characteristics of skeletal
1875 muscle mitochondrial biogenesis induced by moderate-intensity exercise and weight loss in obesity. J Appl
1876 Physiol (1985) 103:21-7.
1877 Menshikova EV, Ritov VB, Toledo FG, Ferrell RE, Goodpaster BH, Kelley DE (2005) Effects of weight loss
1878 and physical activity on skeletal muscle mitochondrial function in obesity. Am J Physiol Endocrinol Metab
1879 288:E818-25.
1880 Miller GA (1991) The science of words. Scientific American Library New York:276 pp. Mitchell P (1961)
1881 Coupling of phosphorylation to electron and hydrogen transfer by a chemi-osmotic type of mechanism.
1882 Nature 191:144-8.
1883 Mitchell P (2011) Chemiosmotic coupling in oxidative and photosynthetic phosphorylation. Biochim Biophys
1884 Acta Bioenergetics 1807:1507-38.
1885 Mitchell P, Moyle J (1967) Respiration-driven proton translocation in rat liver mitochondria. Biochem J
1886 105:1147-62.
1887 Mogensen M, Sahlin K, Fernström M, Glintborg D, Vind BF, Beck-Nielsen H, Højlund K (2007) Mitochondrial
1888 respiration is decreased in skeletal muscle of patients with type 2 diabetes. Diabetes 56:1592-9.
1889 Mohr PJ, Phillips WD (2015) Dimensionless units in the SI. Metrologia 52:40-7.
1890 Moreno M, Giacco A, Di Munno C, Goglia F (2017) Direct and rapid effects of 3,5-diiodo-L-thyronine (T2).
1891 Mol Cell Endocrinol 7207:30092-8.
1892 Morrow RM, Picard M, Derbeneva O, Leipzig J, McManus MJ, Gouspillou G, Barbat-Artigas S, Dos Santos C,
1893 Hepple RT, Murdock DG, Wallace DC (2017) Mitochondrial energy deficiency leads to hyperproliferation of
1894 skeletal muscle mitochondria and enhanced insulin sensitivity. Proc Natl Acad Sci U S A 114:2705-10.
1895 Paradies G, Paradies V, De Benedictis V, Ruggiero FM, Petrosillo G (2014) Functional role of cardiolipin in
1896 mitochondrial bioenergetics. Biochim Biophys Acta 1837:408-17.
1897 Pesta D, Gnaiger E (2012) High-Resolution Respirometry. OXPHOS protocols for human cells and
1898 permeabilized fibres from small biopsies of human muscle. Methods Mol Biol 810:25-58.
1899 Pesta D, Hoppel F, Macek C, Messner H, Faulhaber M, Kobel C, Parson W, Burtscher M, Schocke M, Gnaiger
1900 E (2011) Similar qualitative and quantitative changes of mitochondrial respiration following strength and
1901 endurance training in normoxia and hypoxia in sedentary humans. Am J Physiol Regul Integr Comp Physiol
1902 301:R1078–87.
1903 Price TM, Dai Q (2015) The role of a mitochondrial progesterone receptor (PR-M) in progesterone action.
1904 Semin Reprod Med 33:185-94.
1905 Prigogine I (1967) Introduction to thermodynamics of irreversible processes. Interscience, New York, 3rd
1906 ed:147pp.
1907 Puchowicz MA, Varnes ME, Cohen BH, Friedman NR, Kerr DS, Hoppel CL (2004) Oxidative phosphorylation
1908 analysis: assessing the integrated functional activity of human skeletal muscle mitochondria – case studies.
1909 Mitochondrion 4:377-85. Puntschart A, Claassen H, Jostarndt K, Hoppeler H, Billeter R (1995) mRNAs of
1910 enzymes involved in energy metabolism and mtDNA are increased in endurance-trained athletes. Am J
1911 Physiol 269:C619-25.
1912 Quiros PM, Mottis A, Auwerx J (2016) Mitonuclear communication in homeostasis and stress. Nat Rev Mol
1913 Cell Biol 17:213-26.
1914 Reichmann H, Hoppeler H, Mathieu-Costello O, von Bergen F, Pette D (1985) Biochemical and ultrastructural
1915 changes of skeletal muscle mitochondria after chronic electrical stimulation in rabbits. Pflugers Arch 404:1-
1916 9.
1917 Renner K, Amberger A, Konwalinka G, Gnaiger E (2003) Changes of mitochondrial respiration, mitochondrial
1918 content and cell size after induction of apoptosis in leukemia cells. Biochim Biophys Acta 1642:115-23.
1919 Rich P (2003) Chemiosmotic coupling: The cost of living. Nature 421:583.
1920 Rostovtseva TK, Sheldon KL, Hassanzadeh E, Monge C, Saks V, Bezrukov SM, Sackett DL (2008) Tubulin
1921 binding blocks mitochondrial voltage-dependent anion channel and regulates respiration. Proc Natl Acad Sci
1922 USA 105:18746-51.

1923 Rustin P, Parfait B, Chretien D, Bourgeron T, Djouadi F, Bastin J, Rötig A, Munnich A (1996) Fluxes of
1924 nicotinamide adenine dinucleotides through mitochondrial membranes in human cultured cells. J Biol Chem
1925 271:14785-90.
1926 Saks VA, Veksler VI, Kuznetsov AV, Kay L, Sikk P, Tiivel T, Tranqui L, Olivares J, Winkler K, Wiedemann F,
1927 Kunz WS (1998) Permeabilised cell and skinned fiber techniques in studies of mitochondrial function in
1928 vivo. Mol Cell Biochem 184:81-100.
1929 Salabei JK, Gibb AA, Hill BG (2014) Comprehensive measurement of respiratory activity in permeabilized cells
1930 using extracellular flux analysis. Nat Protoc 9:421-38.
1931 Sazanov LA (2015) A giant molecular proton pump: structure and mechanism of respiratory complex I. Nat Rev
1932 Mol Cell Biol 16:375-88.
1933 Schneider TD (2006) Claude Shannon: biologist. The founder of information theory used biology to formulate
1934 the channel capacity. IEEE Eng Med Biol Mag 25:30-3.
1935 Schönfeld P, Dymkowska D, Wojtczak L (2009) Acyl-CoA-induced generation of reactive oxygen species in
1936 mitochondrial preparations is due to the presence of peroxisomes. Free Radic Biol Med 47:503-9.
1937 Schrödinger E (1944) What is life? The physical aspect of the living cell. Cambridge Univ Press.
1938 Schultz J, Wiesner RJ (2000) Proliferation of mitochondria in chronically stimulated rabbit skeletal muscle--
1939 transcription of mitochondrial genes and copy number of mitochondrial DNA. J Bioenerg Biomembr 32:627-
1940 34.
1941 Simson P, Jepihhina N, Laasmaa M, Peterson P, Birkedal R, Vendelin M (2016) Restricted ADP movement in
1942 cardiomyocytes: Cytosolic diffusion obstacles are complemented with a small number of open mitochondrial
1943 voltage-dependent anion channels. J Mol Cell Cardiol 97:197-203.
1944 Stucki JW, Ineichen EA (1974) Energy dissipation by calcium recycling and the efficiency of calcium transport
1945 in rat-liver mitochondria. Eur J Biochem 48:365-75.
1946 Tonkonogi M, Harris B, Sahlin K (1997) Increased activity of citrate synthase in human skeletal muscle after a
1947 single bout of prolonged exercise. Acta Physiol Scand 161:435-6.
1948 Waczulikova I, Habodaszova D, Cagalinec M, Ferko M, Ulicna O, Mateasik A, Sikurova L, Ziegelhöffer A
1949 (2007) Mitochondrial membrane fluidity, potential, and calcium transients in the myocardium from acute
1950 diabetic rats. Can J Physiol Pharmacol 85:372-81.
1951 Wagner BA, Venkataraman S, Buettner GR (2011) The rate of oxygen utilization by cells. Free Radic Biol Med
1952 51:700-712.
1953 Wang H, Hiatt WR, Barstow TJ, Brass EP (1999) Relationships between muscle mitochondrial DNA content,
1954 mitochondrial enzyme activity and oxidative capacity in man: alterations with disease. Eur J Appl Physiol
1955 Occup Physiol 80:22-7.
1956 Wang T (2010) Coulomb force as an entropic force. Phys Rev D 81:104045.
1957 Watt IN, Montgomery MG, Runswick MJ, Leslie AG, Walker JE (2010) Bioenergetic cost of making an
1958 adenosine triphosphate molecule in animal mitochondria. Proc Natl Acad Sci U S A 107:16823-7.
1959 Weibel ER, Hoppeler H (2005) Exercise-induced maximal metabolic rate scales with muscle aerobic capacity. J
1960 Exp Biol 208:1635–44.
1961 White DJ, Wolff JN, Pierson M, Gemmell NJ (2008) Revealing the hidden complexities of mtDNA inheritance.
1962 Mol Ecol 17:4925–42.
1963 Wikström M, Hummer G (2012) Stoichiometry of proton translocation by respiratory complex I and its
1964 mechanistic implications. Proc Natl Acad Sci U S A 109:4431-6.
1965 Willis WT, Jackman MR, Messer JI, Kuzmiak-Glancy S, Glancy B (2016) A simple hydraulic analog model of
1966 oxidative phosphorylation. Med Sci Sports Exerc 48:990-1000.
1967